REPORT DOCUMENTATION PAGE

Form Approved
OMB No. 0704-0188

1. REPORT DATE *(DD-MM-YYYY)*	2. REPORT TYPE	3. DATES COVERED *(From - To)*
25/11/2009	Final Performance Report	April 2006 - September 2009

4. TITLE AND SUBTITLE
Uncooled Cantilever Microbolometer Focal Plane Arrays with mK Temperature Resolution: Engineering Mechanics for the Next Generation

5a. CONTRACT NUMBER

5b. GRANT NUMBER
FA9550-06-1-0145

5c. PROGRAM ELEMENT NUMBER

6. AUTHOR(S)
Zhang, Xin

5d. PROJECT NUMBER

5e. TASK NUMBER

5f. WORK UNIT NUMBER

7. PERFORMING ORGANIZATION NAME(S) AND ADDRESS(ES)
Dr. Xin Zhang, Associate Professor and Associate Chair, Department of Mechanical Engineering, Boston University, 110 Cummington Street, Boston, MA 02215, USA;
Tel: 617.358.2702, Fax: 617.353.5548, email: xinz@bu.edu

8. PERFORMING ORGANIZATION REPORT NUMBER
AFOSR

9. SPONSORING/MONITORING AGENCY NAME(S) AND ADDRESS(ES)
Dr. B. L. ("Les") Lee, Mechanics of Multifunctional Materials & Microsystems, AFOSR, 875 N. Randolph Street, AFOSR/NA, Suite 325, Room 3112, Arlington, VA 22203, USA; Tel: 703.696.8483, Fax: 703.696.8451, email: ByungLip.Lee@afosr.af.mil

10. SPONSOR/MONITOR'S ACRONYM(S)

11. SPONSORING/MONITORING AGENCY REPORT NUMBER
AFRL-OSR-VA-TR-2012-0433

12. DISTRIBUTION AVAILABILITY STATEMENT

DISTRIBUTION A

13. SUPPLEMENTARY NOTES

14. ABSTRACT

Multilayer cantilever structures are widely applied in micro/nanosystems. Unfortunately, the manufacturability/planarity/reliability has been always inadequate. While much of the understanding regarding the thermomechanical behavior of layered systems derives from experiences in microelectronics, significant differences exist for many micro/nanosysem applications, and these must be well understood to optimize the design of reliable MEMS/NEMS. The overall objectives of this work is to contribute to the scientific understanding of micro- and nano-mechanics of MEMS/NEMS thin film materials so as to develop a revolutionary approach to the design and fabrication of robust, multilayer microcantilever structures and systems for next-generation sensing and imaging applications. This research focuses on understanding the deformation mechanisms in MEMS/NEMS thin film materials, relating these behaviors to the design and analysis of MEMS/NEMS, and applying these principles to improve the performance of the devices/systems in the sub-micron scale. To this end, this research retains a balance between the experimental characterization and theoretical model of small-scale and materials. Because this research leads to a better understanding of micro- and nano- mechanics of multilayer thin films, it will potentially have a broader impact on the enhancement and improvement of a variety of micro/nanosystems for the future needs of the US Air Force.

15. SUBJECT TERMS
MEMS/NEMS, Micro/nanosystems, Micro- and Nano- Mechanics of Multilayer Thin Film Structures, MEMS-based Sensors and Dectors

INSTRUCTIONS FOR COMPLETING SF 298

16. SECURITY CLASSIFICATION OF:			17. LIMITATION OF ABSTRACT	18. NUMBER OF PAGES	19a. NAME OF RESPONSIBLE PERSON
a. REPORT	b. ABSTRACT	c. THIS PAGE		45	19b. TELEPONE NUMBER (*Include area code)*

FINAL PERFORMANCE REPORT TO THE AIR FORCE OFFICE OF SCIENTIFIC RESEARCH

Uncooled Cantilever Microbolometer Focal Plane Arrays with mK Temperature Resolution: Engineering Mechanics for the Next Generation

(Award #: FA9550-06-1-0145)

Final Performance Reports

Xin Zhang

Boston University

Grant Title:	Uncooled Cantilever Microbolometer Focal Plane Arrays with mK Temperature Resolution: Engineering Mechanics for the Next Generation
Grant #:	FA9550-06-1-0145
Reporting Period:	April 2006 – September 2009
PI/Institution/Address:	Dr. Xin Zhang, Associate Professor and Associate Chair, Department of Mechanical Engineering, Boston University, 110 Cummington Street, Boston, MA 02215, USA; Tel: 617.358.2702, Fax: 617.353.5548, email: xinz@bu.edu
Program Manager:	Dr. B. L. ("Les") Lee, Mechanics of Multifunctional Materials & Microsystems, AFOSR, 875 N. Randolph Street, AFOSR/NA, Suite 325, Room 3112, Arlington, VA 22203, USA; Tel: 703.696.8483, Fax: 703.696.8451, email: ByungLip.Lee@afosr.af.mil

Abstract:

Multilayer cantilever structures are widely applied in micro/nanosystems. Unfortunately, the manufacturability/planarity/reliability has been always inadequate. While much of the understanding regarding the thermomechanical behavior of layered systems derives from experiences in microelectronics, significant differences exist for many micro/nanosysem applications, and these must be well understood to optimize the design of reliable MEMS/NEMS. The overall objectives of this work is to contribute to the scientific understanding of micro- and nano- mechanics of MEMS/NEMS thin film materials so as to develop a revolutionary approach to the design and fabrication of robust, multilayer microcantilever structures and systems for next-generation sensing and imaging applications. This research focuses on understanding the deformation mechanisms in MEMS/NEMS thin film materials, relating these behaviors to the design and analysis of MEMS/NEMS, and applying these principles to improve the performance of the devices/systems in the sub-micron scale. To this end, this research retains a balance between the experimental characterization and theoretical model of small-scale and materials. Because this research leads to a better understanding of micro- and nano-mechanics of multilayer thin films, it will potentially have a broader impact on the enhancement and improvement of a variety of micro/nanosystems for the future needs of the US Air Force. (200 words)

Personnel:

Principal Investigator:
Professor Xin Zhang, Associate Professor and Associate Chair, Department of Mechanical Engineering, Boston University, 110 Cummington Street, Boston, MA 02215, USA; Tel: 617.358.2702, Fax: 617.353.5548, email: xinz@bu.edu

Major Ph.D. Students who have fully worked on this project:
Zhiqiang "Jay" Cao, Shusen "Forest" Huang and I-Kuan "Ken" Lin

Zhiqiang "Jay" Cao graduated with a PhD degree in May 2007. His PhD thesis, entitled *Mechanical Behaviors of PECVD Dielectric Films for MEMS Applications*, is available at Boston University Library. If you are interested in getting a copy of the thesis, please contact Prof. Xin Zhang at the address given above.

Shusen "Forest" Huang graduated with a PhD degree in May 2007. His PhD thesis, entitled *Development of Double-Cantilever Infrared Detectors*, is available at Boston University Library. If you are interested in getting a copy of the thesis, please contact Prof. Xin Zhang at the address given above.

I-Kuan "Ken" Lin will graduate with a PhD degree in May 2009. His PhD thesis, entitled *Thermo- and Electromechanics of Multilayer Thin-Film Microstructures for Sensing and Imaging Applications*, will be available at Boston University Library. If you are interested in getting a copy of the thesis, please contact Prof. Xin Zhang at the address given above.

Ph.D. Students who have partially worked/helped on this project:
Hu Tao, Kebin Fan, Bradley Kaanta, and Ping Du

Visiting Scholars, Project-based MS Students, and Undergraduate Researchers who have partially worked on this project:

- Dr. Yan Liu (Visiting Scholar/Research Associate; Self-supported; Now at Entegris)
- Dr. Margarita Marin (Visiting Scholar; Fellowship from Europe; Now back to Europe)
- Axel Gonzalez (MS Graduated in May 2008; Supported by US-Germany Global MS Program; Now in MA-MEMS Industry)
- Richmond Chow (MS Graduated in May 2008; Supported by Industry; Now in BAE)
- Mehmet Ozturk (MS Student; Fellowship from Europe; Plans to Graduate in 2010)
- Emine Balci (MS Student; Fellowship from Europe; Plans to Graduate in 2010)
- George Fraley (Undergraduate Researcher; Now at Northwestern Graduate School)
- George Seamans (Undergraduate Researcher; Now at UC-Berkeley Graduate School)
- Allan Bonhomme-Isaiah (Undergraduate Researcher; Native American/American; Now at BU Graduate School)
- Else Frohlich (Undergraduate Research; Now at BU Graduate School; Won Draper Fellowship for her graduate study in micro/nanosystems)
- Andrew Banfert, Andrew Menard, and James Tumber (Current Undergraduate Researchers)

Publications:

All of journal papers (in PDF format) are available at http://people.bu.edu/xinz. Ph.D. thesis is available at Boston University Library. Should you need any hard copies of these publications, please feel free to contact Prof. Xin Zhang at the address given in the beginning of the report.

([*] denotes graduate students/postdocs supervised by the PI, Prof. Xin Zhang; [#] denotes collaborators of the PI.)

Archival Journal Publications fully or partially supported by this AFOSR Award:

1. I-K Lin[*], P-H Wu, K-S Ou, K-S Chen[#], and **X. Zhang**, "Measurement of Fracture Mechanical Properties of Silicon Oxynitride Films after Rapid Thermal Annealing," submitted/under review, *Thin Solid Films*.

2. I-K Lin[*], Y. Zhang[#], and **X. Zhang**, "Characterization of SiN*x*/Au Biomaterial Microcantilevers with Nanoscale Coating," submitted/under review, *Journal of Micromechanics and Microengineering*.

3. I-K Lin[*], Y. Zhang[#], and **X. Zhang**, "Thermomechanical Behavior and Microstructural Evolution of SiN*x*/Al Bimaterial Microcantilevers," *Journal of Micromechanics and Microengineering*, 19 (8) (2009) 085010.

4. I-K Lin[*], Y-M Liao, Y. Liu, K-S Ou, K-S Chen[#], and **X. Zhang**, "Viscoelastic Mechanical Behavior of Soft Microcantilevers-based Force Sensors," *Applied Physics Letters*, 93 (25) (2008) 251907.

5. I-K Lin[*], Y. Zhang[#], and **X. Zhang**, "The Deformationof Microcantilever-Based Infrared Detectors during Thermal Cycling," *Journal of Micromechanics and Microengineering*, 18 (7) (2008) 075012.

6. Y. Liu[*], I-K Lin[*], and **X. Zhang**, "Mechanical Properties of Sputtered Silicon Oxynitride Films by Nanoindentation," *Materials Science and Engineering A*, 489 (1-2) (2008) 294-301.

7. S. Huang[*], H. Tao[*], I-K Lin[*], and **X. Zhang**, "Development of Double-Cantilever Infrared Detectors: Fabrication, Curvature Control and Demonstration of Thermal Detection," *Sensors and Actuators A: Physical*, 145-146 (2008) 231-240.

8. Z. Cao* and **X. Zhang**, "Nanoindentation Stress-Strain Curves of Plasma Enhanced Chemical Vapor Deposited Silicon Oxide Thin Films," *Thin Solid Films*, 516 (8) (2008) 1941-1951.

9. S. Huang* and **X. Zhang**, "Study of Gradient Stress in Bimaterial Cantilever Structures for Infrared Applications," *Journal of Micromechanics and Microengineering*, 17 (7) (2007) 1211-1219.

10. S. Huang* and **X. Zhang**, "Gradient Residual Stress Induced Elastic Deformation of Multilayer MEMS Structures," *Sensors and Actuators A: Physical*, 134 (1) (2007) 177-185.

11. Z. Cao* and **X. Zhang**, "Nanoindentation Creep of Plasma-Enhanced Chemical Vapor Deposited Silicon Oxide Thin Films," *Scripta Materialia*, 56 (3) (2007) 249-252.

12. Z. Cao* and **X. Zhang**, "Size-dependent Creep Behavior of Plasma-Enhanced Chemical Vapor Deposited Silicon Oxide Films," *Journal of Physics D: Applied Physics*, 39 (23) (2006) 5054-5063.

13. S. Huang*, B. Li*, and **X. Zhang**, "Elimination of Stress-induced Curvature in Microcantilever Infrared Focal Plane Arrays," *Sensors and Actuators A: Physical*, 130-131 (2006) 331-339.

14. Z. Cao* and **X. Zhang**, "Experiments and Theory of Thermally-Induced Stress Relaxation in Amorphous Dielectric Films for MEMS and IC Applications," *Sensors and Actuators A: Physical*, 127 (2) (2006) 221-227.

15. S. Huang* and **X. Zhang**, "Extension of the Stoney Formula for Film-Substrate Systems with Gradient Stress for MEMS Applications," *Journal of Micromechanics and Microengineering*, 16 (2) (2006) 382-389.

Peer-Reviewed Conference Proceeding Publications (Full Paper) fully or partially supported by this AFOSR Award:

1. X. Wang*, S. Yerci, I-K Lin*, L. Dal Negro#, and **X. Zhang**, "Mechanical and Optical Properties of Reactively Sputtered Silicon-rich Silicon Nitride Films," Microelectromechanical Systems--Materials and Devices III, *Materials Research Society Fall Meeting*, Boston, MA, USA, November 30 - December 3, 2009, in press.

2. I-K Lin[*], P-H Wu, K-S Ou, K-S Chen[#], and **X. Zhang**, "The Tunability in Mechanical Properties and Fracture Toughness of Sputtered Silicon Oxynitride Thin Films for MEMS-based Infrared Detectors," Microelectromechanical Systems--Materials and Devices III, *Materials Research Society Fall Meeting*, Boston, MA, USA, November 30 - December 3, 2009, in press.

3. Y. Liu[*], I-K Lin[*], and **X. Zhang**, "Mechanical Properties of Sputtered Silicon Oxynitride Films by Nanoindentation," in Fundamentals of Nanoindentation and Nanotribology IV, edited by Eric Le Bourhis, Dylan J. Morris, Michelle L. Oyen, Ruth Schwaiger, Thorsten Staedler, (*Mater. Res. Soc. Symp. Proc.* Volume 1049, Warrendale, PA, 2007), 1049-AA05-17.

4. S. Huang[*], I-K Lin[*], H. Tao[*], and **X. Zhang**, "Double- Cantilever Micro Infrared Detector: Fabrication, Post-Process Curvature Modification and Thermal Response Characterization," *Proceeding of the 14th International Conference on Solid-State Sensors, Actuators and Microsystems (Transducers '07)*, Lyon, France, June 10-14, 2007, pp. 1601-1604.

5. Z. Cao[*] and **X. Zhang**, "Measurement of Stress-Strain Curves of PECVD Silicon Oxide Thin Films by Means of Nanoindentation," in Processing-Structure-Mechanical Property Relations in Composite Materials, edited by L. Thilly, N. R. Moody, A. Misra, P. M. Anderson, M. Kumar (*Mater. Res. Soc. Symp. Proc.* 977E, Warrendale, PA, 2007), 0977-FF04-23.

6. S. Huang[*] and **X. Zhang**, "Development of Double-Cantilever Infrared Focal Plane Arrays: Fabrication and Post-Process Curvature Modification," in Integrated Nanosensors, edited by B. Ash (*Mater. Res. Soc. Symp. Proc.* 952E, Warrendale, PA, 2007), 0952-F10-03.

7. S. Huang[*] and **X. Zhang**, "Application of Polyimide Sacrificial Layers for the Manufacturing of Uncooled Double-cantilever Microbolometers," in Surface Engineering for Manufacturing Applications, edited by Steve J. Bull, Paul R. Chalker, ShaoChen Chen, Wen Jin Meng, Roya Maboudian (*Mater. Res. Soc. Symp. Proc.* 890, Warrendale, PA, 2006), 0890-Y08-15.

8. Z. Cao[*] and **X. Zhang**, "Influence of Size Effect on Strain Rate Sensitivity and Creep in Plasma-Enhanced Chemical Vapor Deposited Silicon Oxide Films," in Mechanisms of Mechanical Deformation in Brittle Materials, edited by Jodie E. Bradby, Sergei O. Kucheyev, Eric A. Stach, Michael V. Swain (*Mater. Res. Soc. Symp. Proc.* 904E, Warrendale, PA, 2006), 0904-BB04-21.

Conference Presentations fully or partially supported by this AFOSR Award:

1. X. Wang[*], S. Yerci, I-K Lin[*], L. Dal Negro[#], and **X. Zhang**, "Mechanical and Optical Properties of Reactively Sputtered Silicon-rich Silicon Nitride Films," Microelectromechanical Systems--Materials and Devices III, *Presented at Materials Research Society Fall Meeting*, Boston, MA, USA, November 30 - December 3, 2009.

2. I-K Lin[*], P-H Wu, K-S Ou, K-S Chen[#], and **X. Zhang**, "The Tunability in Mechanical Properties and Fracture Toughness of Sputtered Silicon Oxynitride Thin Films for MEMS-based Infrared Detectors," Microelectromechanical Systems--Materials and Devices III, *Presented at Materials Research Society Fall Meeting*, Boston, MA, USA, November 30 - December 3, 2009.

3. I-K Lin[*], K. Zhang, and **X. Zhang**, "Suppression and Modeling of Inelastic Deformation in Multilayer Microcantilevers with Nanoscale Coating," Microelectromechanical Systems--Materials and Devices III, *Presented at Materials Research Society Fall Meeting*, Boston, MA, USA, November 30 - December 3, 2009.

4. I-K Lin[*], K. Fan[*], S. Huang[*], A. Gonzalez[*], Y. Zhang[#], and **X. Zhang**, "Characterization of Gradient Residual Stress Evolution in Bimaterial Microcantilever Structures during Thermal Cycling," *Presented at the ASME International Mechanical Engineering Congress and Exposition (ASME '08)*, Boston, MA, October 31 – November 6, 2008.

5. **X. Zhang**, "Small-Scale Materials and Engineering Mechanics for Next-Generation Micro/Nanosystems," *Presented at the DARPA/MTO Workshop on Materials and Technologies for 21st Century MEMS and NEMS*, Miami, FL, USA, January 8, 2008.

6. Y. Liu[*], I-K Lin[*], and **X. Zhang**, "Mechanical Properties of Sputtered Silicon Oxynitride Films by Nanoindentation," *Presented at Materials Research Society Fall Meeting*, Boston, MA, USA, November 26-30, 2007.

7. I-K Lin[*], Y. Zhang[#], and **X. Zhang**, "Curvature Control of Microcantilever Based Infrared Detectors Using Thermal Loading Method," *Presented at Materials Research Society Fall Meeting*, Boston, MA, USA, November 26-30, 2007.

8. S. Huang*, I-K Lin*, H. Tao*, and **X. Zhang**, "Double- Cantilever Micro Infrared Detector: Fabrication, Post-Process Curvature Modification and Thermal Response Characterization," *Presented at the 14th International Conference on Solid-State Sensors, Actuators and Microsystems (Transducers '07)*, Lyon, France, June 10-14, 2007.

9. Z. Cao* and **X. Zhang**, "Measurement of Stress-strain Curves of PECVD Silicon Oxide Thin Films by Means of Nanoindentation," Processing-Structure-Mechanical Property Relations in Composite Materials, *Presented at Materials Research Society Fall Meeting*, Boston, MA, USA, November 27 - December 1, 2006.

10. S. Huang* and **X. Zhang**, "Development of Double-cantilever Infrared Focal Plane Arrays: Fabrication and Post-process Curvature Modification," Integrated Nanosensors, *Presented at Materials Research Society Fall Meeting*, Boston, MA, USA, November 27 - December 1, 2006.

11. Z. Cao* and **X. Zhang**, "Size Effects in Nanoindentation Creep of Plasma-enhanced Chemical Vapor Deposited Silicon Oxide Films," Size Effects in the Deformation of Materials -- Experiments and Modeling, *Presented at Materials Research Society Fall Meeting*, MA, USA, November 27 - December 1, 2006.

12. S. Huang* and **X. Zhang**, "Characterization of Gradient Residual Stress for Curvature Improvement of MEMS-based Infrared Detector Structures," *Presented at the Optics East 2006*, Boston, MA, USA, October 1-4, 2006.

13. Z. Cao* and **X. Zhang**, "Size-Effects in Nanoindentation Creep of Plasma-Enhanced Chemical Vapor Deposited Silicon Oxide Films," Thin Film & Small Scale Mechanical Behavior, *Presented at the Gordon Research Conference*, Waterville, ME, USA, July 30 - August 4, 2006.

14. S. Huang* and **X. Zhang**, "Theory and Experiments for Gradient Residual Stress in MEMS-based Infrared Detector Structures," *Presented at the IEEE Solid-State Sensor and Actuator Workshop (Hilton Head '06)*, Hilton Head Island, SC, USA, June 4-8, 2006.

15. Z. Cao* and **X. Zhang**, "Length-scale Effect on Nanoindentation Creep in Plasma-Enhanced Chemical Vapor Deposited Silicon Oxide Films," *Presented at the IEEE Solid-State Sensor and Actuator Workshop (Hilton Head '06)*, Hilton Head Island, SC, USA, June 4-8, 2006.

Ph.D. Thesis fully or partially supported by this AFOSR Award:

1. I-Kuan "Ken" Lin*, "Thermo- and Electromechanics of Multilayer Thin-Film Microstructures for Sensing and Imaging Applications," *Ph.D. Thesis*, 2006-. (Anticipated 2010)

2. Shusen "Forest" Huang*, "Development of Uncooled Cantilever Microbolometer Focal Plane Arrays with mK Temperature Resolution," *Ph.D. Thesis*, May 2007.

3. Zhiqiang "Jay" Cao*, "Mechanical Behaviors of PECVD Dielectric Films for MEMS Applications," *Ph.D. Thesis*, May 2007.

Honors/Awards:

- Shusen "Forest" Huang: Received Ph.D. in May 2007.
- Zhiqiang "Jay" Cao: Received Ph.D. in May 2007.
- Hu "Tiger" Tao: Boston University Provost Award (2008).
- Bradley Kaanta: Boston University Technology Development Award (2008).
- I-Kuan "Ken" Lin: Best Poster Award at 2008 ASME International Mechanical Engineering Congress and Exposition (Boston, MA, October 31 – November 6, 2008). Only five awards were granted and Ken was honored a Third-Place Prize.
- Hu "Tiger" Tao: Best Poster Award at 2008 Photonics Center Symposium. Only three awards were granted and Tiger was honored a First-Place Prize.
- Bradley Kaanta: Boston University Nanoscience & Nanotechnology Award (2009).
- Kebin Fan: Boston University Photonics Center Berman Future of Light Prize Award (2009).
- Kebin Fan: Boston University Photonics Center Senior Research Assistantship Award (2009)
- Dr. Xin Zhang: Invited presentation at DARPA Workshop on Materials and Technologies for 21st Century MEMS and NEMS, January 2008.
- Dr. Xin Zhang: Invited presentation at NSF Workshop on Grand Challenges for Bio-Nano Integrated Manufacturing for the Year 2020, April 2008.
- Dr. Xin Zhang: Invited presentation at the 5th US-Korea Forum on Nanotechnology, April 2008.
- Dr. Xin Zhang: Invited presentation at National University of Singapore, Singapore, April 2008.
- Dr. Xin Zhang: Invited presentation at Keio University, Japan, April 2008.
- Dr. Xin Zhang: Invited presentation at Draper Lab, Cambridge, June 2008.
- Dr. Xin Zhang: Invited presentation at NSF Workshop on MNS Horizon 2040, June 2009.
- Dr. Xin Zhang: Became an Invitee of National Academy of Engineering (recognized as one of the top engineers in the country between the ages of 30-45) (2007).
- Dr. Xin Zhang: Received Schlumberger Award for her excellence and leaderships in MEMS/NEMS research (2008).
- Dr. Xin Zhang: Named the inaugural Distinguished Faculty Fellow, a five-year appointment given to tenured College of Engineering faculty who is on a clear trajectory toward exemplary leadership career in all dimensions of science and engineering (2008).
- Dr. Xin Zhang: Boston University Dean's Catalyst Award (2009).

Introduction

In the late 1970s, MEMS emerged as a discipline based on the use of silicon IC materials and fabrication processes to produce non-electrical devices that could interface with IC signal-processing circuits. Initial product successes for MEMS included pressure sensors, accelerometers, and optical systems based on movable mirrors. With the invention of surface micromachining, actuation as well as sensing became a designable goal in MEMS. Surface micromachining also stimulated designs with materials other than silicon, often incorporated as thin films. These new materials provided new degrees-of-freedom exploiting important material properties such as piezoelectricity, bi-layer thermal effects, and magnetism. Many other materials properties such as magnetostrictive, electrostrictive, piezoresistive, shaped-memory effects, photoconductance, and photoluminescence are also being explored for various future MEMS/NEMS applications. Of equal importance to materials and their properties are appropriate technologies and knowledge to enable designers to effectively exploit these new materials in successful MEMS/NEMS products. A basic understanding of new materials and technologies that allow material properties to be accurately determined, quality control of material deposition systems, and compatibility of materials with other fabrication processes are all important topics that require careful consideration.

Thin Films and Micro/Nanosystems:

Thin film materials have been widely used in microelectronic devices and packages; MEMS; and surface coatings with thermal, mechanical, tribological, environmental, optical, electrical, magnetic, or biological functionalities. This research is primarily motivated by multilayer thin film microstructures in MEMS devices and systems, which as microsensors and microactuators have found numerous applications in aerospace, automotive, communications, optics, biotechnology, and so on. Thin films in MEMS must satisfy a large set of rigorous chemical, structural, mechanical, and electrical requirements. Excellent adhesion, low residual stress, low pin-hole density, good mechanical strength, and chemical resistance may be required simultaneously. It is well known that as manufacturing operations approach micron scale, or even submicron/nanoscale, material properties of thin film materials generally differ from their bulk counterparts. It is thus crucial to understand the unique properties of the MEMS thin film materials, in order to better design, characterize, and manufacture successful MEMS structures and devices for the next generation.

Mechanical Behavior of Thin Films:

Of particular interest are the mechanical responses of the thin film materials, which will be the focus of this research. This is first because, as the acronym suggests, MEMS typically integrate mechanical components with the electronics required for control. In other words, it most often contains a movable part of some sort, which creates a special need for the understanding of the micromechanics of the device. Secondly, many deleterious effects during MEMS fabrication and integration, such as excessive wafer bowing, film cracking, delamination, and defects formation etc., are related to the

residual stress in the films and are mechanical in nature. Last but not least, the long-term reliability of MEMS relies on the time-dependent mechanical properties of the thin films, such as creep and fatigue, etc. This is especially important for those MEMS structures and devices working in "harsh environments", i.e. high temperature, high stress level, and/or high strain rates, etc. Examples include pressure sensors for aerospace applications, micro heat engines and related components, etc.

Multilayer Thin Film Material Systems:

Multilayer thin film material systems abound in MEMS applications, serving both passive and active structural roles. In these many applications dimensional control is a critical issue. Surface micromachined mirrors, for example, require optically flat surfaces; less than 10% of a wavelength variation across the mirror's surface. Holographic data storage and optical beam steering for display applications need reflective surfaces free of optical phase distortion to increase the signal-to-noise ratio, minimize cross-talk, and keep the system in focus. This level of optical flatness is difficult to achieve due to curvature commonly seen in micromachined mirrors composed of several different material layers. For other applications, such as RF MEMS, cantilever and bridge-like structures are used to make electrostatic switches. It is important to control deformation of these large areas of thin actuator structures in order to achieve desired deflection versus voltage relationships, on/off switching times, and RF frequency response. To obtain the necessary thermal expansion mismatch in bi-layer actuators, one film is typically a metal and the other a material with a much lower thermal expansion coefficient such as a glass or ceramic. An inherent characteristic of such bi-layer material structures is that misfit strains between the layers (for example, due to intrinsic processing stresses or thermal expansion mismatch between the materials upon a temperature change) lead to stresses in the layers and deformation of the structures. Innovative designs and layering arrangements have led to microactuators capable of deforming both in and out of the plane of the bi-layer, providing three-dimensional motion. Such actuators have been used for many purposes including RF switches, optical positioning, accelerometers, and 3-D microassembly.

MEMS vs. Microelectronics – differences in behavior:

Numerous studies have elucidated the basic thermomechanical response of layered plates when subjected to temperature changes or other sources of misfit strains between the layers. These have come in the context of many technological applications, the most common being structural composite materials and thin film/thick substrate systems for microelectronics applications. In this case one layer (the thin film) is much smaller than the other (the thick substrate). If subjected to a 100 °C temperature change, the maximum deflection would about two percent of the thickness. In MEMS applications the layer thicknesses are not only small relative to in-plane dimensions, but they are often comparable to each other. If subjected to a 100 °C temperature change, the maximum deflection would be about six times of the thickness. The deformation behavior of structures with microelectronics applications is usually within the linear regime. However for MEMS applications, the deformation behavior are much more complicated and often

requires the usage of geometric nonlinearity theory. While much of the understanding regarding the thermo-mechanical behavior of layered systems derives from experiences in microelectronics, significant differences exist for many MEMS applications, and these must be well understood to optimize the design of reliable MEMS.

Applications / Aspects	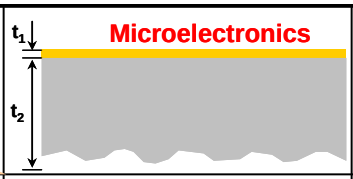 Microelectronics	 MEMS
Film thickness	**$t_1 << t_2$ t_1=0.5 μm, t_2=500 μm**	**comparable t_1=0.5 μm, t_2=1.5 μm**
Temperature change	**- 100°C**	**- 100°C**
Deflection (of total thickness)	**2%**	**6 times**
Stresses across the thickness	**Uniform (150 MPa)**	**Stress gradient (~70MPa)**
Stresses over the in-plane	**Uniform**	**Nonuniform**
Curvature	**Uniform (0.9 m^{-1})**	**Nonuniform (~550 m^{-1})**
Stress vs. curvature	**Stoney formula**	**Complicated**
Geometric nonlinearity Bifurcation	**No**	**Yes**

Technical Objectives:

The importance of successful development of MEMS and its descendent NEMS is clear to our community, which is also aware of the need for leading researchers in the field to identify promising new materials and structures for MEMS/NEMS and to master and characterize technologies that will qualify these materials and structures for robust and reliable system applications.

The overall objectives of this work is to contribute to the scientific understanding of micro- and nano- mechanics of MEMS/NEMS thin film materials so as to develop a revolutionary approach to the design and fabrication of robust, multilayer microcantilever structures and systems for next-generation sensing and imaging applications for the future needs of the US Air Force. To this end, this research will retain a balance between the experimental characterization and theoretical model of multifunctional MEMS structures and materials.

Approaches:

- Microsystem design and fabrication.
- Residual stress evolution and thermomechanical behavior of thin films
- Deformation mechanisms in multilayer microcantilever structures during cyclic thermal loading and isothermal holding (reliability issue)
- Post-processing curvature modification
- Suppressing the inelastic deformation using nano-scale coating

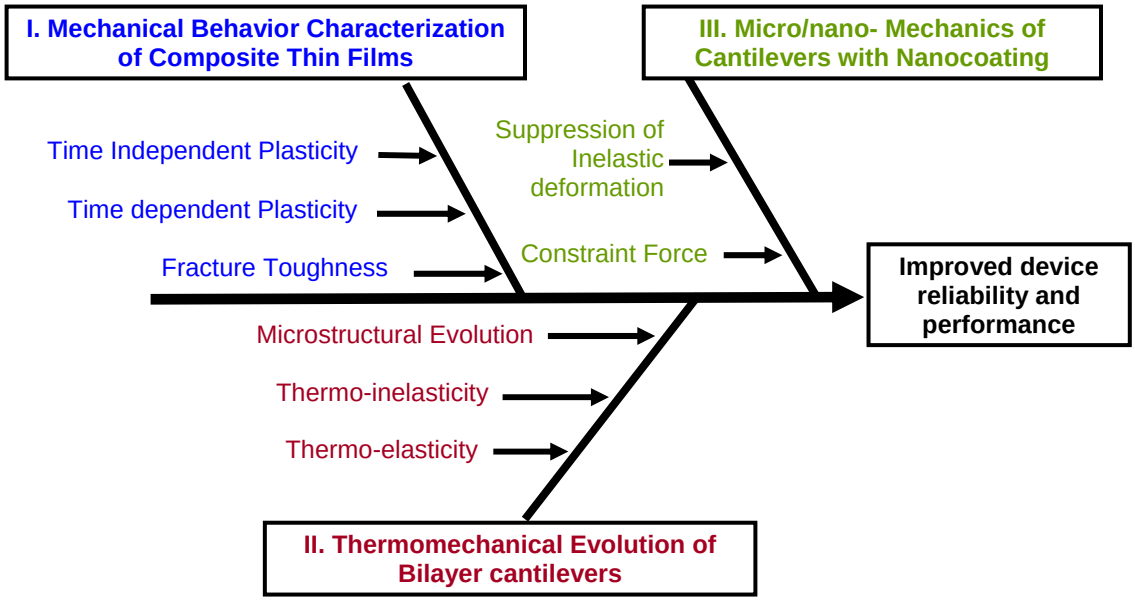

Expected Benefits and Future Potentials:

Devices:

- Infrared detectors can be designed in different configurations to suit the specific need. The US Air Force has shown great interest in this technology. Applications range from aerospace to scientific, industrial, civil, medical, military and many others.
- Recent advances in MEMS would enable a significant development of uncooled infrared detectors. By not necessitating a cooling system, infrared detectors would require 20 times less power, be 10 to 100 times smaller in size, and cost 10 times less than cooled detectors.

Mechanics and Materials:

- Multilayer cantilever structures are widely applied in micro/nanosystems. Unfortunately, the manufacturability, planarity and reliability have been always inadequate. While much of the understanding regarding the thermomechanical behavior of layered systems derives from experiences in microelectronics, significant differences exist for many micro/nanosysem applications, and these must be well understood to optimize the design of reliable MEMS.
- The overall goal of this research is to understand the deformation mechanisms in MEMS thin film materials, relate these behaviors to the design and analysis of MEMS, and apply these principles to improve the performance of the devices in the sub-micron scale.
- This research will lead to a better understanding of the relationship between structures and properties of free-standing thin film materials, which will potentially have a broader impact on other microelectronics and MEMS structures and devices for the future needs of the US Air Force.

- Broadly speaking, this research would also help to identify more effective means for engaging the materials science and engineering mechanics community in work important to continuing advances in micro/nanosystems. Our vision is to transform the science and engineering community's capacity to probe multilayer thin film materials at micro and nano scales by developing both new theoretical models and experimental methodologies. These characterization techniques and platforms will allow scientists to ask profound and previously intractable questions related to MEMS/NEMS thin film materials, and to obtain quantitative empirical answers with resolution sufficient to characterize thin film materials in small scales.

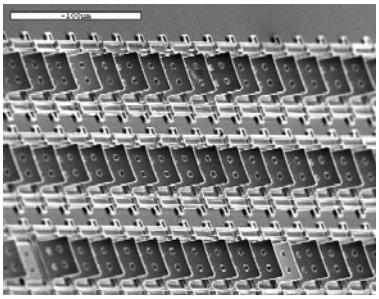

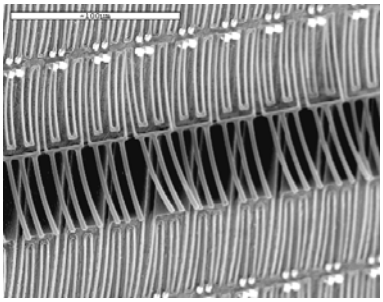

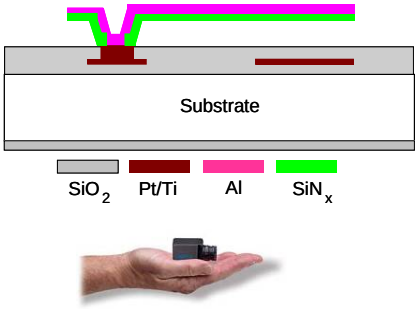

Accomplishment/New Findings I:
Elimination of Stress-induced Curvature in Microcantilever Infrared Focal Plane Arrays

Major Publication:
S. Huang, B. Li, and **X. Zhang**, "Elimination of Stress-induced Curvature in Microcantilever Infrared Focal Plane Arrays," *Sensors and Actuators A: Physical*, 130-131 (2006) 331-339.

Abstract:
This paper reports an approach to eliminating stress-induced curvature in microcantilever-based infrared focal plane arrays (FPAs). Using a combination of argon ion beam machining and rapid thermal annealing (RTA), we successfully modified curvatures of free-standing SiN*x*/Al bimaterial FPAs. The SiN*x*/Al FPAs were fabricated using a surface micromachining technique with polyimide as a sacrificial material. The as-fabricated FPAs were concavely curved because of the imbalanced residual stresses in the two materials. To modify the FPAs curvature, first, Ar ions with energies of 500 eV was used, which sputter etched PECVD SiN*x* at a rate of 4 nm/min, and 20 min of ion beam machining reduced the FPAs curvature from −1.92 to −0.96mm^{-1}. Then based on the investigation on the thermomechanical behavior of both the e-beam Al and PECVD SiN*x* films during the thermal cycling, RTA was proposed to further modify the FPAs curvature. It is found that 5 min of RTA at 375 °C resulted in flat FPAs with acceptable curvatures (<0.10mm^{-1}).

Selected Figures/Results:

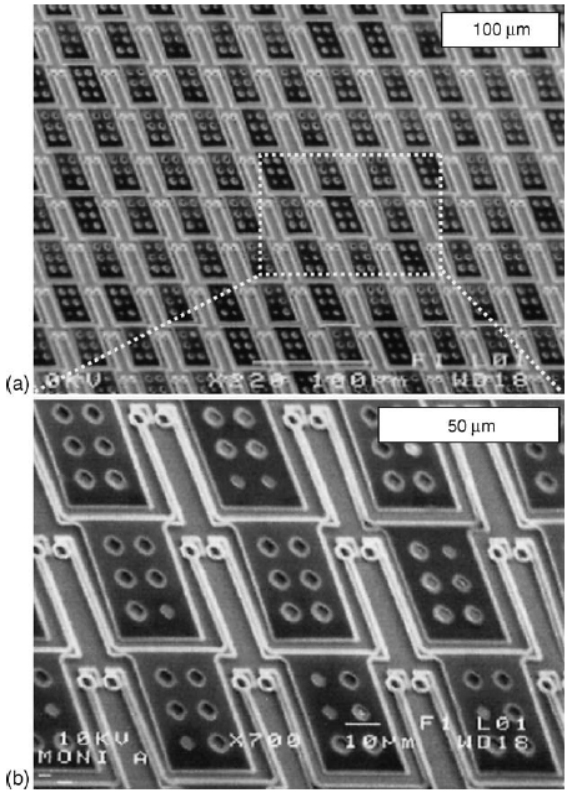

Fig. I-1: (a) An SEM image of a part of bimaterial SiN*x*/Al cantilever IR FPAs. (b) A close-up view showing that the as-fabricated pixels were concavely curved because of the imbalanced residual stresses in the two materials.

Notes: Process flow for the fabrication of SiN*x/Al cantilever IR FPAs. (a) A 2.5µm-thick polyimide was spin coated on a Si substrate and cured at 350 ◦C, followed by the deposition of a 500 nm-thick PECVD SiOx. (b) The polyimide was patterned by RIE with the SiOx as the hard mask. (c) After the removal of the SiOx, a 200 nm-thick e-beam Al and a 200 nm-thick PECVD* SiN*x were deposited. (d) The* SiN*x was patterned by RIE with a mixture of SF6 and He, followed by the patterning of the Al by phosphorous acid. (e) The biomaterial* SiN*x/Al FPAs were released upon the removal of the sacrificial polyimide.*

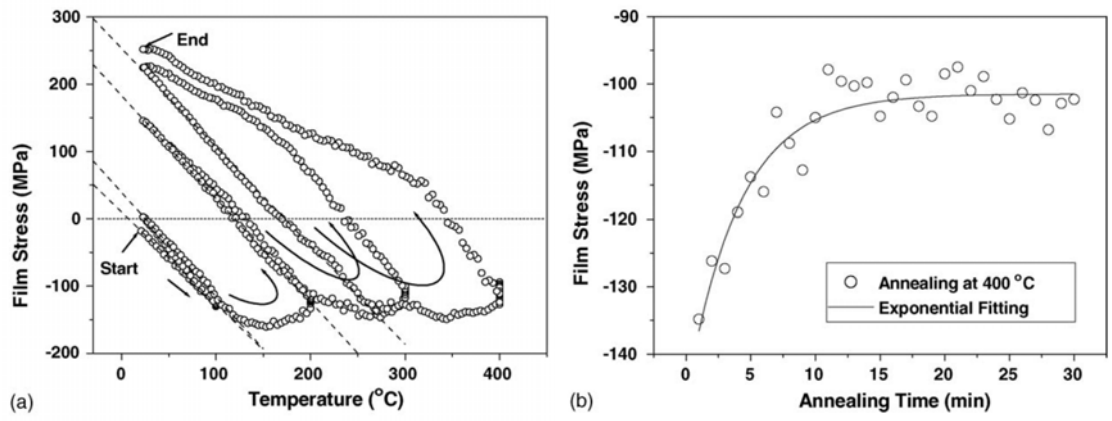

Fig. I-2: (a) Biaxial film stress response of a 200 nm-thick e-beam Al to the thermal cycling. (b) The stress development with time during the annealing at 400 °C.

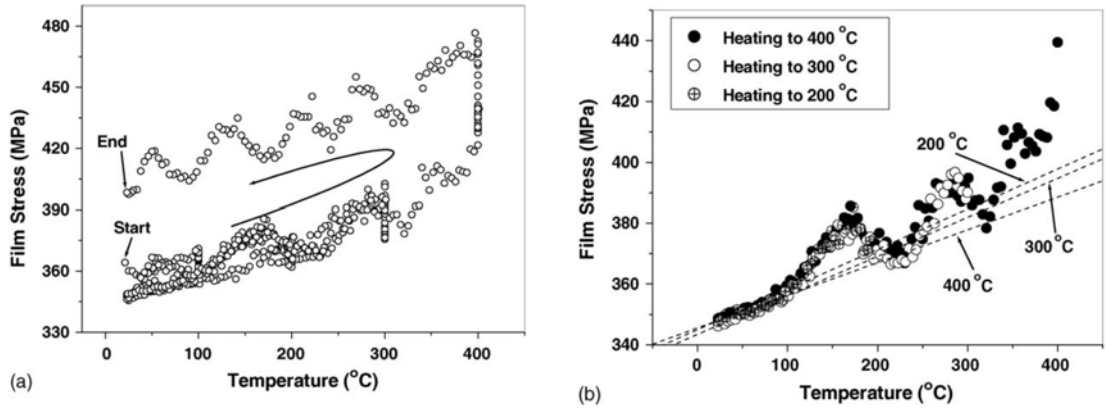

Fig. I-3: (a) Biaxial film stress response of a 200 nm-thick PECVD SiN*x* to the thermal cycling. (b) The stress response of the SiN*x* during the heating processes to 200, 300, and 400 °C.

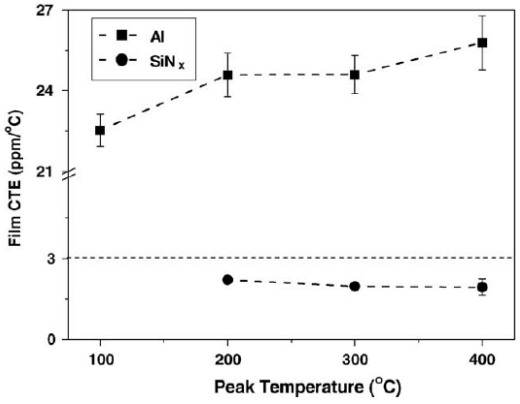

Fig. I-4: CTEs of 200 nm-thick e-beam Al films and 200 nm-thick PECVD SiN*x* films as a function of peak temperature.

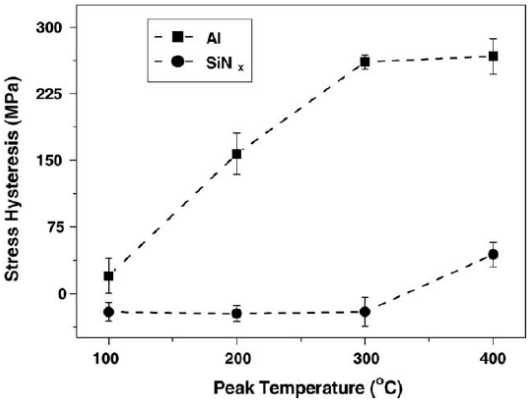

Fig. I-5: Stress hysteresis of the 200 nm-thick e-beam Al and the 200 nm-thick PECVD SiN*x* films under different peak temperatures varying from 100 to 400 °C.

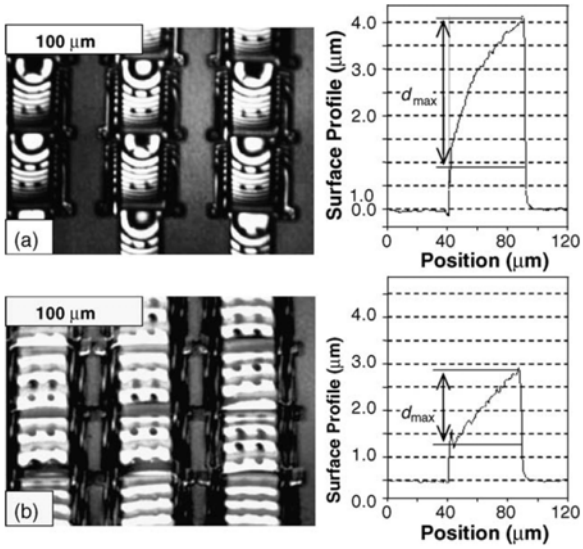

Fig. I-6: Interference fringes and surface profiles showing that the SiN*x*/Al cantilever IR FPAs were less curved after 20 min of Ar ion beam machining.

Concluding Remarks:

Cantilever infrared detectors have the potential of reaching an NETD approaching the theoretical limit if the residual stress-induced curvature of SiN*x*/Al FPAs can be effectively eliminated. As such, the reduction of the FPAs curvature is currently a major research effort in the development of cantilever infrared detectors. In this paper, the SiN*x*/Al FPAs were fabricated using a low-temperature surface micromachining technique with polyimide as a sacrificial material and the as-fabricated FPAs were concavely curved. A thorough understanding of the stress response to thermal cycling and annealing is a prerequisite to predicting the behavior of such bimaterial devices during processing, operation as well as post-processing curvature modification.

The thermomechanical behavior of both e-beam Al and PECVD SiN*x* films were explored in our work. To modify the FPAs curvature, Ar ion beam machining was used. Ar ions with energies of 500 eV sputter etched PECVD SiN*x* at a rate of 4 nm/min. It was found that 20 min of ion beam machining reduced the curvature of the FPAs from -1.92 to -0.96 mm^{-1}, while 40 min of ion beam machining resulted in the delamination of the bimaterial structures. In addition, based on the investigation on the stress hysteresis of the Al and SiN*x* films during the thermal cycling, various RTA treatments were performed to further modify the FPAs curvature. It was observed that 5 min of RTA at 375 °C resulted in flat FPAs with acceptable curvatures (<0.10mm^{-1}).

In summary, we demonstrated that a combination of ion beam machining and RTA techniques can be used effectively to eliminate the residual stress-induced curvatures in cantilever-based infrared arrays. Such an approach also shines a light on a certain possibility to control “unwanted” initial curvatures in many other kinds of free-standing MEMS structures, such as micromirror arrays.

Accomplishment/New Findings II:
Extension of the Stoney Formula for Film-Substrate Systems with Gradient Stress for MEMS Applications

Major Publication:
S. Huang and **X. Zhang**, "Extension of the Stoney Formula for Film-Substrate Systems with Gradient Stress for MEMS Applications," *Journal of Micromechanics and Microengineering*, 16 (2) (2006) 382-389.

Abstract:
Using the Stoney formula and its modifications, curvature-based techniques are gaining increasingly widespread application in evaluating the stress in a film on a substrate. In principle, the formula applies only when the stress is uniform throughout the film thickness. The main purpose of this paper is to extend the Stoney formula when the residual strain in the film is no longer uniform, but dependent on the z position. To achieve this goal, a general theory was introduced for the elastic deformation of an arbitrary, multilayered system. By practicing this general theory, we used a polynomial function to describe the gradient stress in a film, and contributions by different elements of the polynomial to both the curvature and the bending strain were derived. A finite element simulation for a typical film–substrate structure was then carried out, leading to the verification of the theory developed in this paper. In the discussion section, we explored the relation between the surface curvature and the bending curvature as well as the difference between the stress in the constrained planar state and that in the relaxed state. In addition, the accuracy of the simplified formula, using thin film approximation, was evaluated. Finally, a SiN*x*-Al MEMS structure was studied by using the formula in this paper.

Concluding Remarks:

The widely used Stoney formula and its modifications hold for a film–substrate system only when the film stress is uniformly distributed through the thickness. The present study develops an exact solution for the elastic deformation of such a film– substrate system due to the arbitrarily distributed constrained stress in the film. When the initial constrained stress in the film is completely characterized by various experimental ways, the developed relationship can be used not only to determine the deformation of a film–substrate system but also to give the profiles of the bending stress (strain) and the residual stress (strain) in the thickness direction. The FE simulation of a p+ silicon–silicon structure was then carried out, resulting in the results that agree well with the theoretical calculation. While the curvature measured with a laser scanning system has a different meaning from the bending curvature, this study also shows that, quantitatively, there is little difference between the surface curvature and the bending curvature. However, in general, there is much difference between the constrained stress and the average residual stress even when the constrained stress in the film is uniform throughout the thickness. In addition, the stress–curvature relation in SiN*x*-Al infrared structures was studied demonstrating that, compared to the original Stoney formula and its previous modifications, the theory developed in this paper can deal with more complex issues.

Accomplishment/New Findings III:
Gradient Residual Stress Induced Elastic Deformation of Multilayer MEMS Structures

Major Publication:
S. Huang and **X. Zhang**, "Gradient Residual Stress Induced Elastic Deformation of Multilayer MEMS Structures," *Sensors and Actuators A: Physical*, 134 (1) (2007) 177-185.

Abstract:
Multilayered structures are widely used as sensing or actuating components in MEMS devices. Since the thin films of multilayered structures are always subject to residual stresses, it is important to model the relation between these residual stresses and the resultant elastic deformation. The main purpose of this paper is to explore two different approaches to addressing this issue when the residual stress in each thin film is not necessarily uniform throughout the thickness. These two approaches are first briefly introduced and then used to arrive at identical solutions for a monolayer cantilever and a bilayer cantilever, both with arbitrary residual strain distributions throughout the thickness. The analytical formulas for a bilayer cantilever are further verified by the numerical simulation of a special case. After the discussion on the errors induced by assuming the gradient residual strains in the bilayer cantilevers are uniform, the relation between the bending plane and the neutral plane in bilayer cantilevers is also explored. Finally, we present an approach to characterizing residual stresses in thin films by using micromachined bilayer cantilevers in conjunction with the theory developed in this paper.

Concluding Remarks:

A lot of research has been done on the residual strain-induced elastic deformation of multilayered structures. In this present contribution we explored two different approaches to relating the gradient residual stresses in thin films of such a multilayered structure to the resultant elastic deformation. In both approaches we used a polynomial function to describe the arbitrary residual strain profile in a thin film. The first approach can be regarded as a top-down approach. In this approach, after the extensional stiffness coefficient, the flexural–extensional coupling stiffness coefficient, the flexural stiffness coefficient, the axial force, and the bending moment of the structure were obtained, a simple, general theory yielded the reference strain and the bending curvature simultaneously. On the other hand, the second approach started from the analysis of individual layers. The deformation strain of each layer was determined by the gradient residual strain in this layer and also the internal forces and the internal moments applied by its adjacent layers. Since all of the layers had the same bending curvature and the continuity requirement of the deformation strain at the interface between two neighboring layers must be satisfied, we obtained a series of linear functions to derive the bending curvature and all of the internal forces and internal moments. After that, the solutions to the profiles of the deformation strain and then the true strain throughout the thickness of the structure were obtained. In this article, employing both approaches to explore the monolayer cantilevers and the bilayer cantilevers led to identical solutions and also demonstrated that the both approaches are conceptually correct, efficient, and user-

friendly. It should be noted that both approaches could also address the elastic deformation induced by an external force or an external moment. It should also be noted that the second approach could deal with a multilayer structure consisting of thin films with various width when the maximum width is still much smaller than the length. The FE simulation results of the special case in the discussion section agreed well with analytical prediction, leading to the verification of the formulas developed in this article. The discussion on the errors induced by ignoring the gradient residual strains in bilayer cantilevers indicated that it is necessary to consider the gradient residual strains for some cases. By exploring monolayer and bilayer cantilevers, the bending plane and the neutral plane not only showed to have different physical behaviors but also to be different in quantity for most cases. Finally, the employment of the theory developed in this paper led to the formulas for characterizing residual stresses in thin films by using micromachined cantilevers.

Accomplishment/New Findings IV:
Study of Gradient Stress in Bimaterial Cantilever Structures for Infrared Applications

Major Publication:
S. Huang and **X. Zhang**, "Study of Gradient Stress in Bimaterial Cantilever Structures for Infrared Applications," *Journal of Micromechanics and Microengineering*, 17 (7) (2007) 1211-1219.

Abstract:
Bimaterial SiN*x*/Al infrared cantilever structures are always initially curved because of the imbalanced residual stress in the two layers. Their performance and functionality are therefore significantly decreased. A thorough study of the residual stress (strain) has then become a key issue in the development of bimaterial SiN*x*/Al cantilever structures. In the curvature-based approach to the film stress, the residual strain is derived from the measured curvature based on certain assumptions on the distribution of the residual strain in the thickness direction. Previous models for a bimaterial cantilever structure, however, are not sufficient to characterize the residual strain in bimaterial SiN*x*/Al infrared structures. The main goal of this paper is to investigate gradient residual strain in bimaterial SiN*x*/Al infrared structures. To achieve this goal, the relationship between the residual strain and bending curvature is developed with the assumption that the residual strain in each layer is linearly distributed rather than uniform throughout the thickness. The profile of the gradient strain is then derived from the curvatures measured during the continuous etching of the top-most SiN*x* in the bimaterial cantilevers. The derived residual strain can then be inverted to predict curvature change further in the etching process. This paper demonstrates that a linear assumption of the residual strain yields a stronger agreement with the measured data in comparison to previously used models. In addition, several factors that may affect measurement accuracy are discussed at the end of the paper.

Concluding Remarks:

The bimaterial SiN*x*/Al infrared cantilever structures are always initially curved because of the imbalanced residual stress in the two layers. Their performance and functionality are therefore significantly decreased. In this present contribution, we develop a new model and also conduct etching experiments to explore the gradient residual stress (strain) in bimaterial SiN*x*/Al cantilever infrared structures. In the curvature-based approach to the film strain, the residual strain is derived from the measured curvature based on certain assumptions on the distribution of the residual strain in the thickness direction. Previous models for a bimaterial cantilever structure, however, are not enough to characterize the residual strain in bimaterial SiN*x*/Al infrared structures. Therefore, in this paper the residual strain in both layers is assumed to be linear gradient and a new model is presented to relate the residual strain to the resultant bending curvature. In our experiments, the bending curvature is obtained from the measured surface profiles along the etching process. The strain profile is then derived from the measured curvatures of the first three data points. Furthermore, the derived strain profile is reversely used to predict the curvature change during the further etching process after the first three data points.

The curvature prediction based on our new model yields a significantly stronger agreement with the measured data in comparison with the results based on previous models. In addition, higher-order polynomial assumptions (n = 2, 3, 4) on the residual strain in the SiNx layer are also examined in this paper. However, these assumptions do not result in better curvature predictions in comparison with the result from the linear assumption (n = 1). Since the curvature in our work is derived from the surface profiles using a two-order polynomial fitting, several factors that may affect the measurement accuracy are also examined. This paper demonstrates that R-squared of the two-order polynomial fitting is very close to 1, and therefore the measurement error from the surface roughness can be ignored. Measurement errors may also be induced by the etching rate difference along the length direction because the cantilever structure is initially curved. The maximum etching rate difference is estimated to be less than 3%. Using a modified etching rate, the strain profile is derived and then used to predict the curvature change. However, there is no significant difference from the previous prediction without the etching rate modification. In conclusion, the present study provides a more appropriate modeling of the residual strain-induced deformation of bimaterial SiNx/Al infrared structures. The investigation of the gradient residual strain in the thickness direction will benefit post-processing curvature control of SiNx/Al infrared FPAs.

Summary of Accomplishment/New Findings II, III, and IV:

Multilayer Mechanics
(Review on Previous Work)

- Single layer cantilevers
  - ➢ Linear stress
    - A. Fang, 1995
    - B. Greek, 1999
  - C. Arbitrary stress distribution (Yang, 1995)
- A film-substrate system with uniform stress in the film
  - D. Thin-film approximation (Stoney, 1909)
  - ➢ Thin-film approximation breaks
    - E. First-order approximation (Brenner, 1949)
    - F. Second-order approximation (Aktinson, 1995)
    - • Complete solution
      - G. Freud,1999
      - H. Klein, 2000
- Bimaterial cantilevers
  - I. Uniform stresses in both layers (Chu, 1993)
  - ➢ Uniform stress in one layer and linear stress in another
    - J. Min, 2000
    - K. Hou, 2004
- Multilayer structure
  - ➢ Uniform stress in each layer
    - L. Townsend, 1987
    - M. Marcus, 1996
    - N. Pulskamp, 2003
    - O. Malzbender, 2004
  - P. Linear stress in one layer and uniform stress in other layers (Freund,1996)

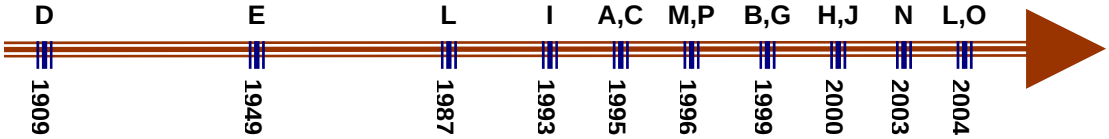

Multilayer Mechanics
(Motivations and Assumptions)

- **What's the curvature?**
  - **Multilayered structure**
  - **Arbitrary thickness ratio**
  - **Gradient stress in each layer**
- **Assumptions**
  - The thickness is much smaller than the length and all layers have the same length and width;

- The material is homogeneous, isotropic, and linearly elastic;
- The edge effects near the periphery are inconsequential;
- The strains and the rotations are elastic and infinitesimally small.

Multilayer Mechanics
(A Top-down Approach)

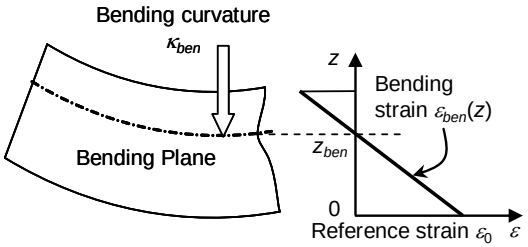

Gradient residual strain

$$\varepsilon_{res,i}(z) = \sum_{k=0}^{\infty} \varepsilon_{res,i,k} \left[(z - z_i)/h_i\right]^k$$
$$(z_i \le z \le z_{i+1})$$

Bending strain $\varepsilon_{ben}(z) = \varepsilon_0 - \kappa_{ben} z$

Total strain $\varepsilon_{def}(z) = \varepsilon_{res}(z) + (\varepsilon_0 - \kappa_{ben} z)$

Total potential energy

$$U(\varepsilon_0, \kappa_{ben}) = \frac{WL}{2} \int_0^h E(z)\left[\varepsilon_{def}(z)\right]^2 dz$$

Equilibrium requirement

$\partial U / \partial \kappa_{ben} = 0$

$\partial U / \partial \varepsilon_0 = 0$

Bending curvature & reference strain

$$\begin{bmatrix} \varepsilon_0 \\ \kappa_{ben} \end{bmatrix} = \frac{1}{B^2 - AD} \begin{bmatrix} DN - BM \\ BN - AM \end{bmatrix}$$

$$(A, B, D) = \int_0^h E(z)\left(1, z, z^2\right) dz$$

$$(N, M) = \int_0^h E(z)\varepsilon_{res}(z)(1, z)\, dz$$

Multilayer Mechanics
(A Bottom-up Approach)

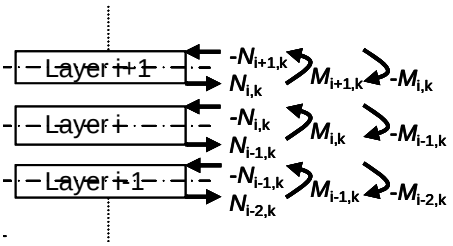

1) Internal forces and moments

Δ Gradient residual strain

$$\varepsilon_{res,i}(z) = \sum_{k=0}^{\infty} \varepsilon_{res,i,k} \left[(z - z_i)/h_i\right]^k$$
$$(z_i \le z \le z_{i+1})$$

2) Beam theory for each layer $\kappa_{ben,k} = \frac{M_{i,k}}{E_i I_i}$

3) Bending moment

$$M_{i,k} = \frac{E_i b h_i^2 k \varepsilon_{res,i,k}}{2(k+1)(k+2)} + \frac{(N_{i-1,k} + N_{i,k})h_i}{2} + (M_i - M_{i-1})$$

4) Total strain throughout the thickness

$$\varepsilon_{def,i,k}(z) = \frac{\varepsilon_{res,i,k}}{k+1} + \frac{N_{i-1,k} - N_{i,k}}{E_i h_i b} - \kappa_{ben,k}\left(z - z_i - \frac{h_i}{2}\right)$$

5) Continuity requirement at the interface

$\varepsilon_{def,i,k}(z_{i+1}) = \varepsilon_{def,i+1,k}(z_{i+1})$

Multilayer Mechanics
(Top-down & Bottom-up Approaches)

- The two approaches result in exactly same results for the same cases.\
- The results from our approaches agree well with previous work by others listed here.
- Our methods can be used for more advanced, complicated situations.
- M: A 2n-pair epitaxial structure with periodic distribution of mismatch strain (Marcus, 1996, J. Appl. Phys. 79 8364)

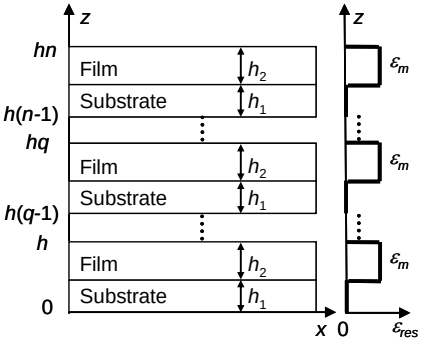

$$\kappa = \frac{1}{h_1}\frac{6(1+r)\gamma r\varepsilon_m}{n^2(1+\gamma r)^2(1+r)^2+(2\gamma r^2+\gamma r-r-2)(1-\gamma)r}$$

$$\varepsilon_0 = \frac{-n^2(1+r)^2(1+\gamma r)+3n(1+r)^2-(1-\gamma)(1+2r)r}{n^2(1+r)^2(1+\gamma r)^2+(2\gamma r^2+\gamma r-r-2)(1-\gamma)r}\gamma r\varepsilon_m$$

Multilayer Mechanics
(Extension of Stoney's Formula)

A film-substrate system with uniform stress in the film with thin-film approximation (Stoney,1909)

$$\kappa_{ben} = \frac{6\gamma r\varepsilon_f}{h_s}$$

Thin-film approximation breaks

- First-order approximation (Brenner,1949)
- Second-order approximation (Aktinson,1995)
- Complete solution (Freud,1999 and Klein, 2000)

$$\kappa_{ben} = \frac{1}{h_s}\frac{6\gamma r\varepsilon_f}{1+4\gamma r+6\gamma r^2+4\gamma r^3+\gamma^2 r^4}$$

No thin-film assumption; No uniform residual stress assumption

$$\kappa_{ben} = \frac{1}{h_s}\frac{6\gamma r}{1+4\gamma r+6\gamma r^2+4\gamma r^3+\gamma^2 r^4}$$

$$\sum_{k=0}^{\infty}\frac{\gamma r^2 k+2r(k+1)+k+2}{(k+1)(k+2)}\varepsilon_{res,k}$$

$$\varepsilon_0 = \frac{2\gamma r}{1+4\gamma r+6\gamma r^2+4\gamma r^3+\gamma^2 r^4}$$

$$\sum_{k=0}^{\infty}\frac{(k-1)\gamma r^3+3k\gamma r^2+3(k+1)r+k+2}{(k+1)(k+2)}\varepsilon_{res,k}$$

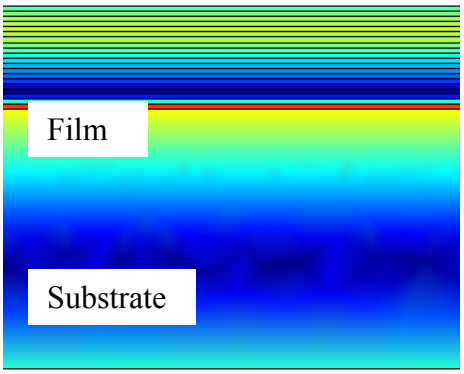

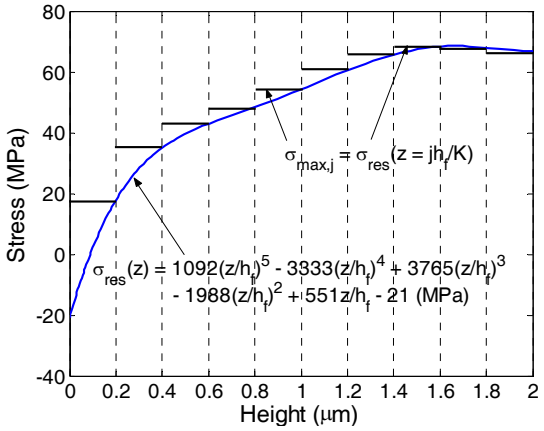

Yang et al., Appl. Phys. Lett. 67 912

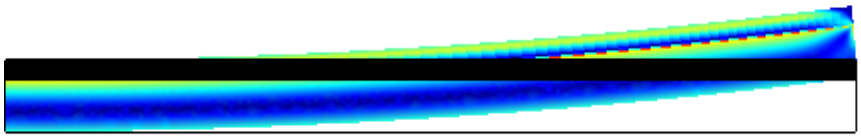

■ Curvature

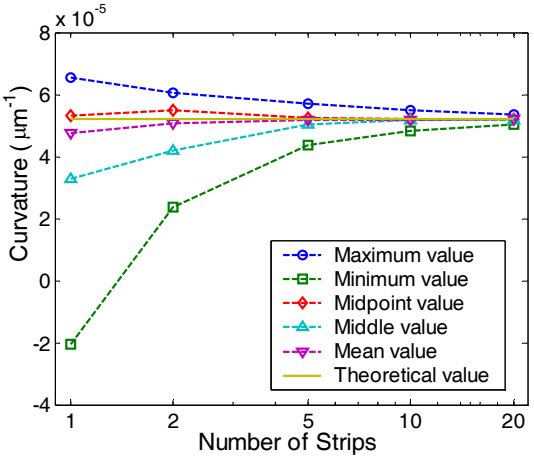

■ Total stress

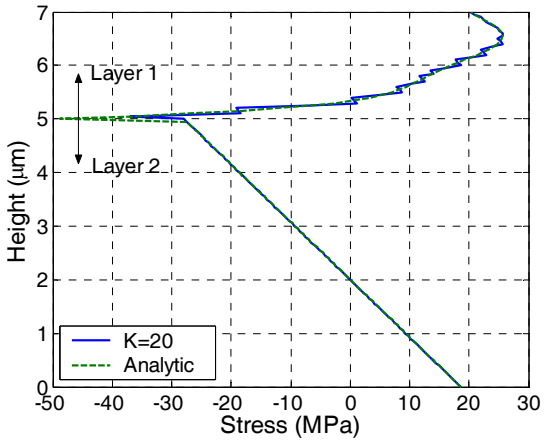

Multilayer Mechanics
(Stress Profile in IR Structure)

- Uniform stresses in both layers (Chu, 1993)
- Uniform stress in one layer and linear stress in another (Min, 2000 and Hou, 2004)
- RIE: SF6 + He = 20sccm + 30sccm, 75 mTorr, 110W

→ Etching rate: 109 nm/min

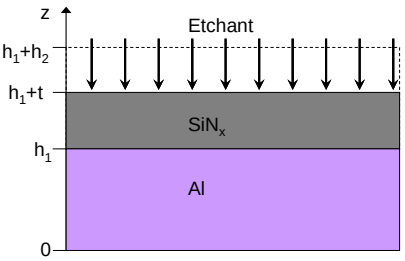

- Uniform stresses in both layers (Chu, 1993)

  → Mismatch strain $\varepsilon_{res,2,0}$-$\varepsilon_{res,1,0}$

$$\kappa_{ben} = \frac{6\gamma r(1+r)\varepsilon_{mis}}{h_1(1+4\gamma r+6\gamma r^2+4\gamma r^3+\gamma^2 r^4)}$$

- Uniform stress in one layer and linear stress in another (Min, 2000 and Hou, 2004)

  → Mismatch strain $\varepsilon_{res,2,0}$-$\varepsilon_{res,1,0}$

  → Gradient strain $\varepsilon_{res,1,1}$

- Linear stresses in both layers

  → Mismatch strain $\varepsilon_{res,2,0}$-$\varepsilon_{res,1,0}$

  → Gradient strain $\varepsilon_{res,1,1}$, $\varepsilon_{res,2,1}$

$$\kappa_{ben} = \frac{\begin{array}{l}6\gamma r(1+r)\varepsilon_{mis}+\gamma r(3+4r+\gamma r^2)\varepsilon_{res,2,1}r/r_0\\ +(1-2\gamma r-3\gamma r^2)\varepsilon_{res,1,1}\end{array}}{h_1(1+4\gamma r+6\gamma r^2+4\gamma r^3+\gamma^2 r^4)}$$

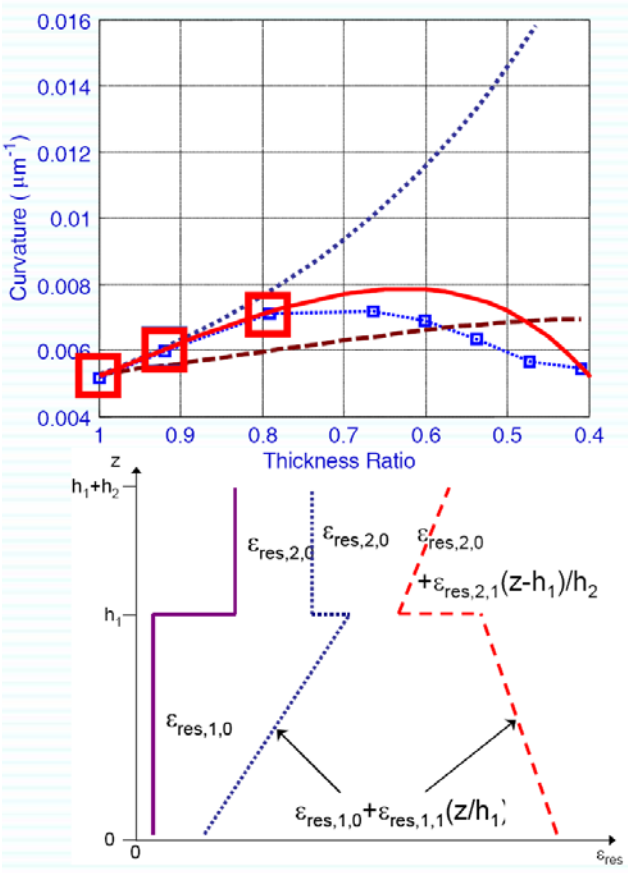

Accomplishment/New Findings V:
Development of Double-Cantilever Infrared Detectors: Fabrication, Curvature Control and Demonstration of Thermal Detection

Major Publication:
S. Huang, H. Tao, I-K Lin, and **X. Zhang**, "Development of Double-Cantilever Infrared Detectors: Fabrication, Curvature Control and Demonstration of Thermal Detection," *Sensors and Actuators A: Physical*, 145-146 (2008) 231-240.

Abstract:
This paper reports the recent progress on the development of double-cantilever infrared (IR) detectors, including the fabrication, the post-process curvature control, and also the first-time demonstration of thermal detection using capacitive-based IR focal plane arrays (FPAs). In this work, simplified double-cantilever IR FPAs based on bimaterial SiN*x*/Al and Al/SiN*x* cantilevers are fabricated using a surface micromachining module with polyimide as the sacrificial material. Thermal-cycling experiments of both 200 nm-thick Ebeam Al and 200 nm-thick PECVD SiN*x* films reveal that the residual stresses in IR materials can be significantly modified by thermal annealing. Therefore, an engineering approach to flattening IR FPAs is developed by using rapid thermal annealing (RTA). This article also demonstrates the thermal detection of cantilever IR FPAs using commercialized weak capacitance readout IC.

Selected Figures/Results:

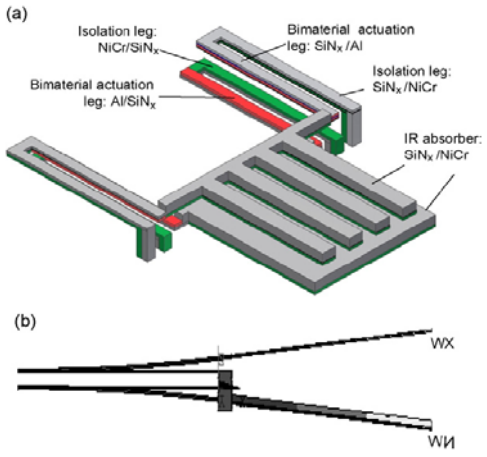

Fig. V-1: (a) The 3D view showing the major components and materials of a pixel in the double-cantilever IR FPAs and (b) the front-side view from FEM simulations shows that upon temperature increase, the top cantilever will bend upward while the bottom one downward.

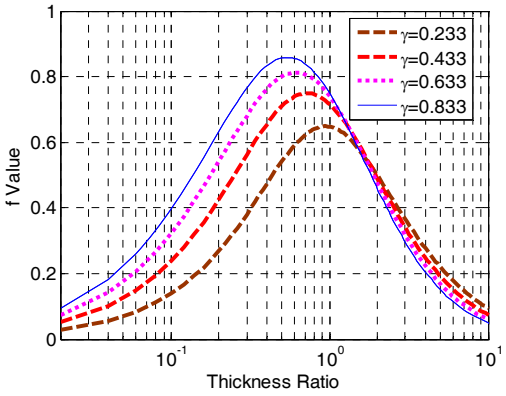

Fig. V-2: f-values for various modulus ratios as a function of the thickness ratio.

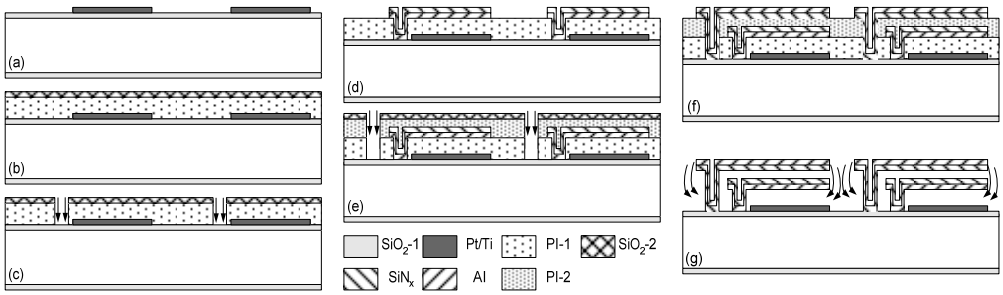

Fig. V-3: Fabrication process of the double-cantilever microbolometer FPAs: (a) 150 nm-thick Pt/Ti wires and pads by standard lift-off process on thermal-oxidized silicon wafers, (b) spin-on coating and curing of 2.5μm -thick polyimide and deposition of a 500 nm-thick etching mask layer of PECVD SiO_2, (c) etching of SiO_2 by RIE with SF6 and He and anisotropic etching of polyimide by RIE with O_2, (d) the bottom bimaterial cantilever of a 200 nm-thick PECVD SiN*x* layer and a 200 nm-thick Ebeam Al layer, (e) the second sacrificial layer of 1-μm thick polyimide, (f) the top bimaterial cantilever of a 200 nm-thick Ebeam Al layer and a 200 nm-thick PECVD SiN*x* layer, and (g) release of the microbolometer FPAs by isotropic etching of both polyimide layers with O_2 plasma.

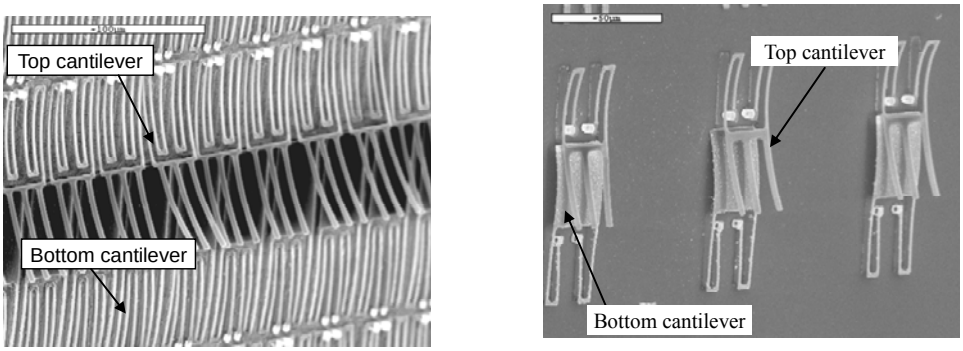

(a) (b)

Fig. V-4: The as-fabricated bottom cantilevers are curved downward to the substrate, while the top ones are curved upward.

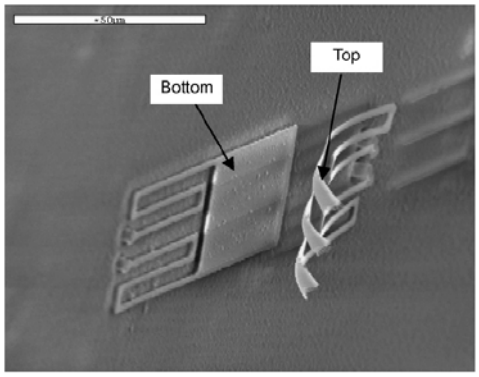

Fig. V-5: The release of the bottom cantilever has not started while the top one has been completely released.

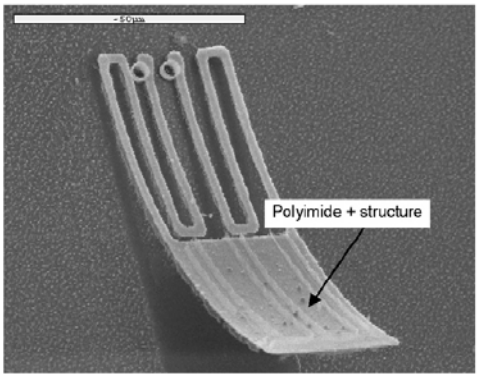

Fig. V-6: Because of high temperature during the release process, the bottom cantilever and the bottom polyimide layer delaminate from the substrate.

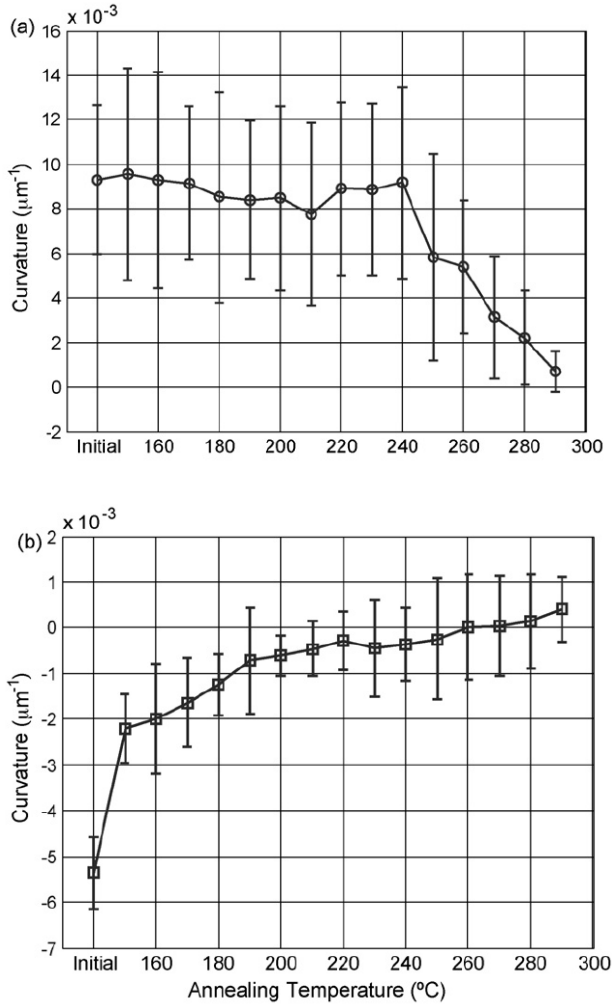

Fig. V-7: RTA treatment is demonstrated to be a valid method for the post-process curvature modification: the curvature change as a function of annealing temperature for top cantilevers (a), and bottom cantilevers (b) in double-cantilever IR FPAs.

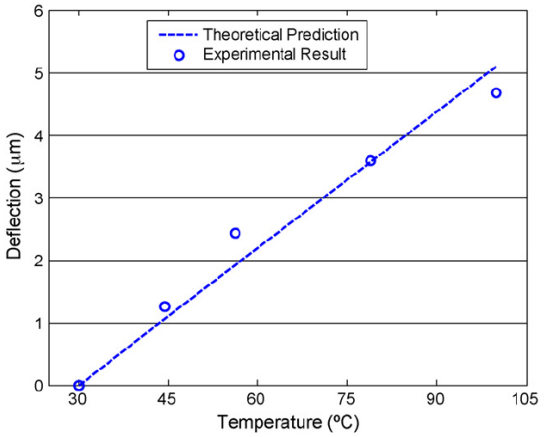

Fig. V-8: Thermal–mechanical response of simplified IR structures.

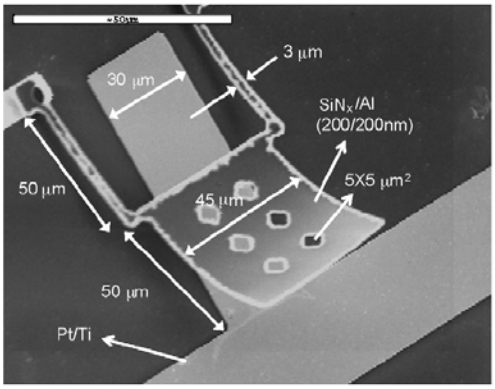

Fig. V-9: Geometry of the single pixel in the thermal-detection experiment.

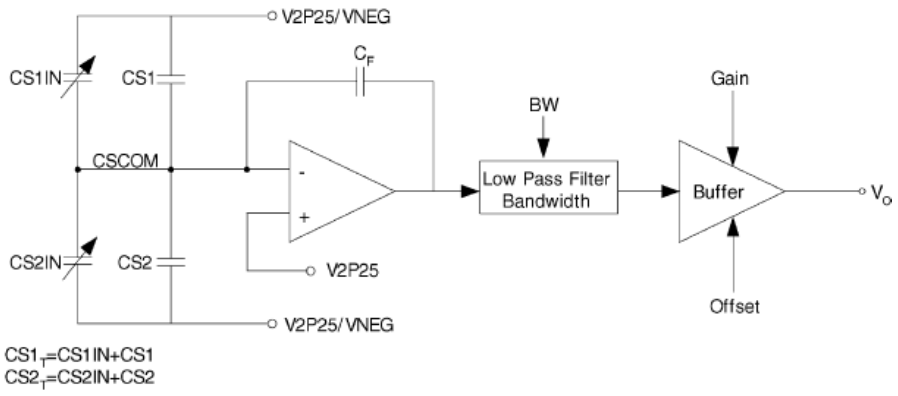

Fig. V-10: The block diagram of the MS3110 IC.

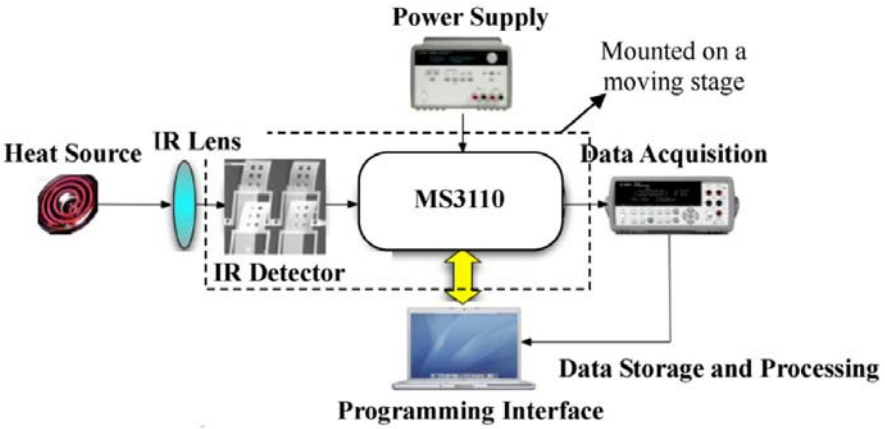

Fig. V-11: Testing system for proof-of-concept demonstration of thermal detection using a single-cantilever IR dector.

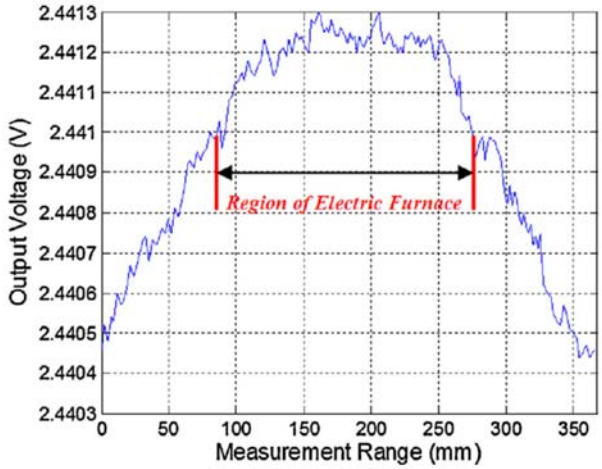

Fig. V-12: Thermal-electric response of a simplified single-cantilever IR detector when a burning furnace is scanned using a moving stage.

Concluding Remarks:

In summary, we successfully developed of a surface-micromachining module with polyimide as the sacrificial material and PECVD SiN*x* and Ebeam Al as the structure materials for the fabrication of simplified single- and double-cantilever FPAs. This microfabrication technique can be readily used for the fabrication of a wide variety of complex free-standing multilayer MEMS structures. But as mentioned in the paper, the final release by O_2 plasma is extremely time-consuming. The etching holes should be designed in both top and bottom cantilever structures to accelerate the release process. Also, in order to avoid damages or delamination of the FPAs from the substrate, the temperature should be carefully monitored and controlled during the release process. Athorough understanding of the stress response to thermal cycling and annealing is a prerequisite to predicting the behavior of such bimaterial devices during processing, operation as well as post-processing curvature modification. The thermomechanical behavior of both Ebeam Al and PECVD SiN*x* films were explored in our work. Based on the investigation on the stress hysteresis of the Al and SiN*x* films during the thermal cycling, double-cantilever FPAs with curvatures less than $0.001 mm^{-1}$ are achieved by using the post-process RTA treatments. It should be pointed that although RTA is an effective method to control FPAs curvature, it is unlikely to get both flat top cantilevers and flat bottom cantilevers after the same RTA treatment. For example, we found that the average curvature of top cantilevers reaches minimum at 290 °C, that of the bottom cantilevers, however, reaches minimum at 270 °C. Therefore, better temperature control during the thermal annealing is highly recommended in the future work. Finally, the feasibility of thermal detection of IR FPAs is demonstrated by using a testing setup developed in this work. It should be pointed out that vacuum package is eventually required for the realization of high sensitivity and low NETD. Therefore, the thermal detection experiment in this work inherently features a low sensitivity. Also, one of the major advantages of using the capacitive readout for cantilever-based IR detectors is the possible integration with the signal readout IC. Although this is not demonstrated in our work, the integration approach has been explored by other researchers.

Accomplishment/New Findings VI:
Mechanical Properties of Sputtered Silicon Oxynitride Films by Nanoindentation

Major Publication:
Y. Liu, I-K Lin, and **X. Zhang**, "Mechanical Properties of Sputtered Silicon Oxynitride Films by Nanoindentation," *Materials Science and Engineering A*, 489 (1-2) (2008) 294-301.

Abstract:
Silicon oxynitride (SiON) has received a great deal of attention in micro-electro-mechanical system (MEMS) integration due to its composition-dependent tunability in optical, electronic and mechanical properties. In thiswork, silicon oxynitride films with different oxygen and nitrogen content were deposited by RF magnetron sputtering. Energy dispersive X-ray (EDX) spectroscopy and Fourier-transform infrared (FT-IR) spectroscopy were employed to characterize the SiON films with respect to stoichiometric composition and atomic bonding structure. Time-dependent plastic deformation (creep) of SiON films were investigated by depth-sensing nanoindentation at room temperature. Young's modulus and indentation hardness were found correlated with the nitrogen/oxygen ratio in SiON films. Results from nanoindentation creep indicated that plastic flow was less homogenous with increasing nitrogen content in film composition. Correspondingly, a deformation mechanism based on atomic bonding structure and shear transformation zone (STZ) plasticity theory was proposed to interpret creep behaviors of sputtered SiON films.

Selected Figures/Results:

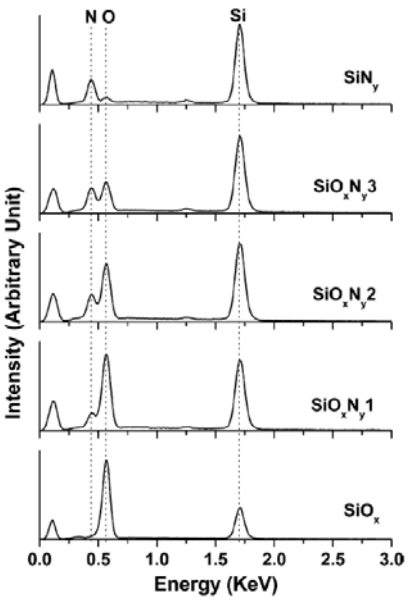

Fig. VI-1: EDX spectra of the SiON films.

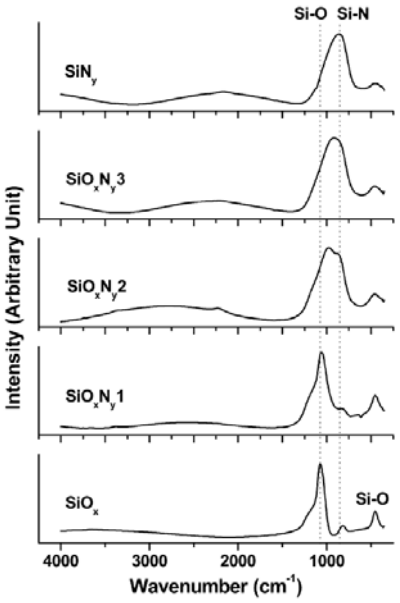

Fig. VI-2: MIR FT-IR absorbance spectra of the SiON films.

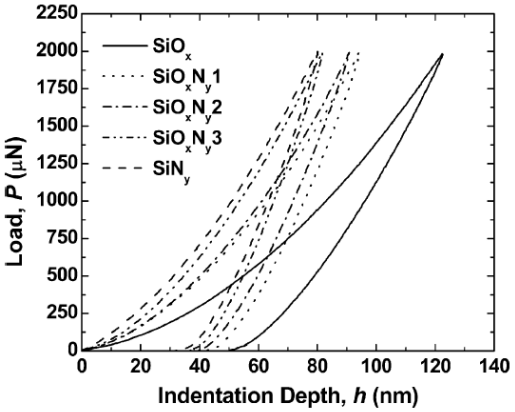

Fig. VI-3: Load–displacement (*P*–*h*) curves of the SiON films in the constant rate of loading nanoindentation experiments.

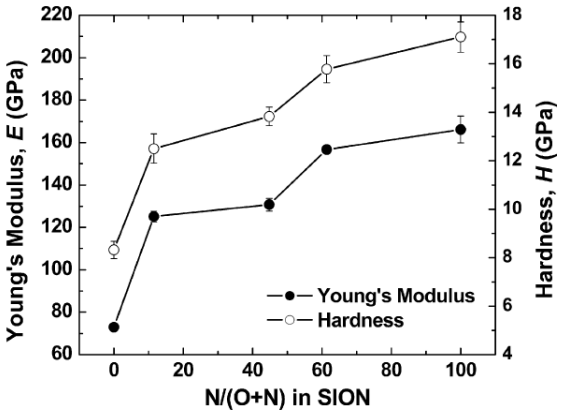

Fig. VI-4: Young's modulus and indentation-hardness of the SiON films as a function of the nitrogen content [N/(O + N)].

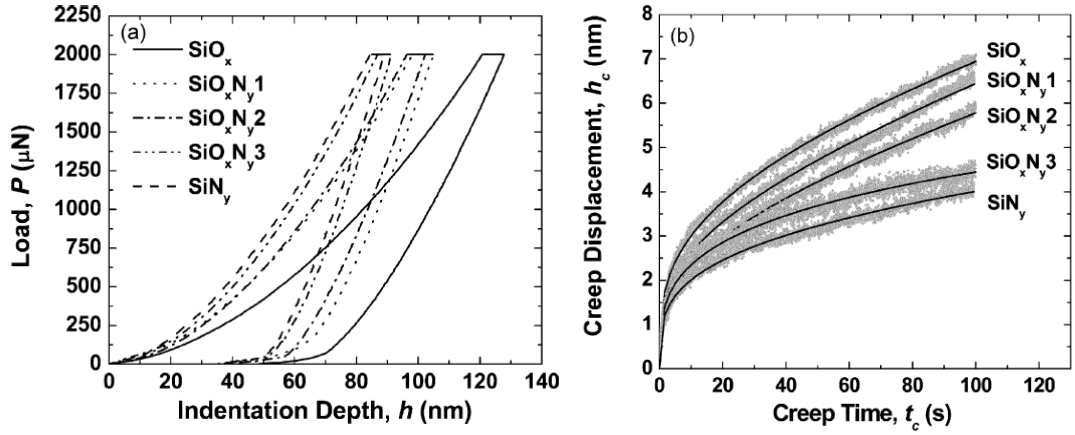

Fig VI-5: Nanoindentation creep of the SiON films: (a) load–displacement (*P*–*h*) curves and (b) creep displacement $h_c(h-h_0)$ vs. creep time $t_c(t-t_0)$ curves (solid scatters) with corresponding fittings (solid lines).

Young's modulus and indentation-hardness of the SiON films

Specimen	Young's modulus, *E* (GPa)	Hardness, *H* (GPa)
SiO_x	73.01	8.32
SiO_xN_y1	125.09	12.50
SiO_xN_y2	130.75	13.83
SiO_xN_y3	156.67	15.78
SiN_y	166.13	17.10

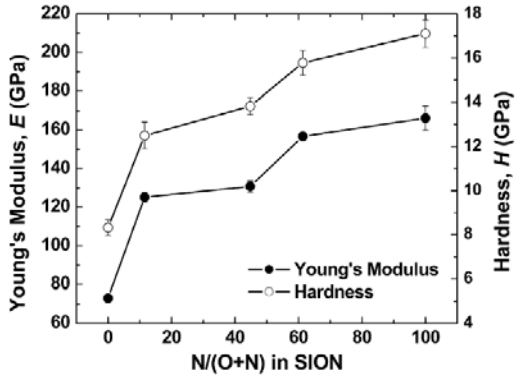

Fig. VI-6: Young's modulus and indentation-hardness of the SiON films as a function of the nitrogen content [N/(O + N)].

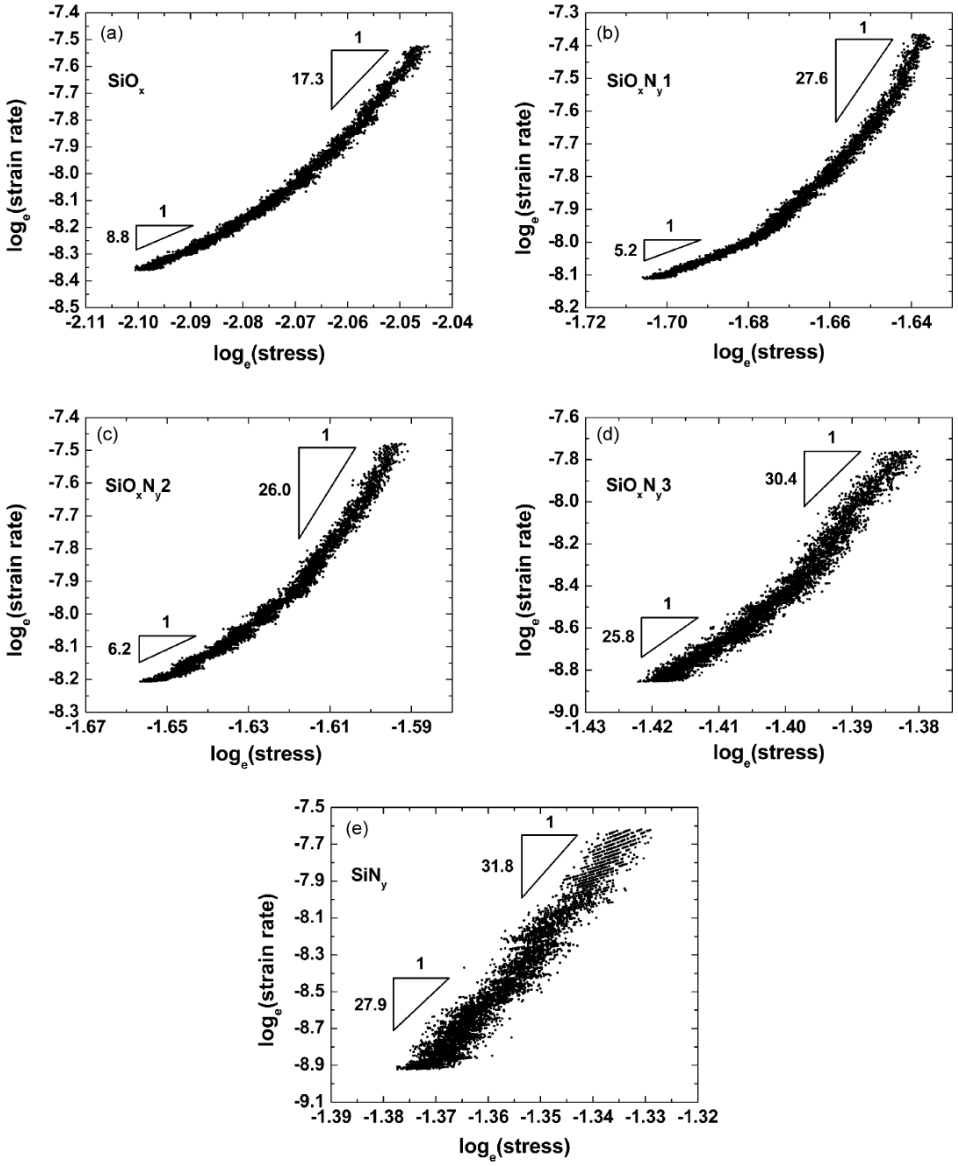

Fig. VI-7: Logarithm relations of strain rate and applied stress [log(˙ε)−log(σ)] in steady-state nanoindentation creep for the SiON films: (a) SiO*x*; (b)SiO*x*N*y*1; (c) SiO*x*N*y*2; (d) SiO*x*N*y*3 and (e) SiN*y*.

Plastic Flow of Amorphous Material:

- In amorphous materials, plastic flow is mediated by the activation and rearrangement of "shear transformation zones (STZs)".
- The STZ clusters in the SiOxNy films could be comprised of a combination of Si-O, Si-N, and Si-O-N units.
- STZs are blocked by the rigid Si-N-Si bridging bonds in movement.
- The creep behaviors of SiON illustrated a strong correlation with content of oxygen and nitrogen in composition.

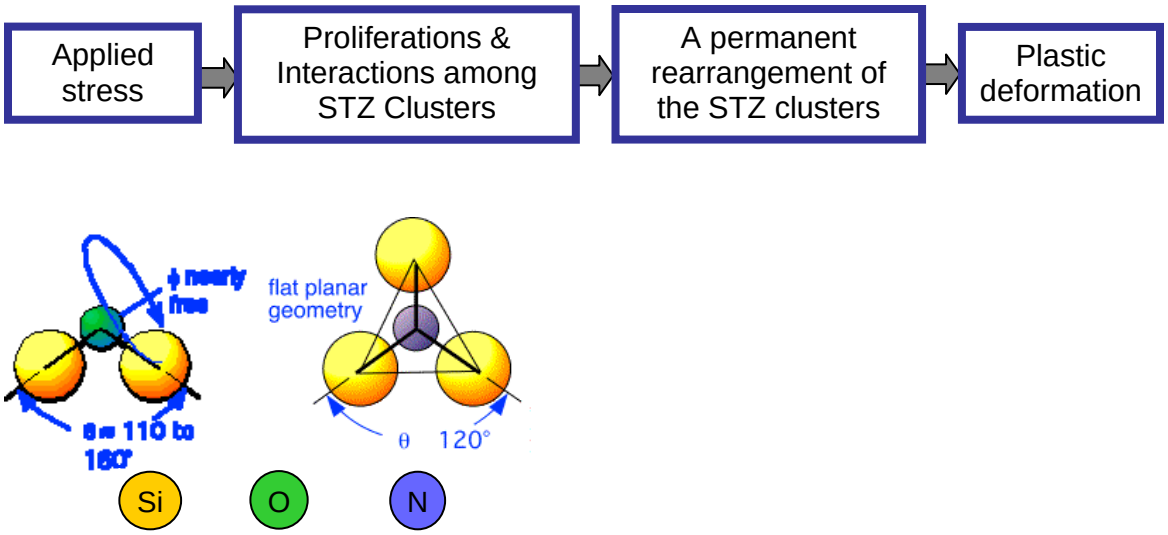

Concluding Remarks:

Amorphous SiON films with varied composition of oxygen and nitrogen content ranging from SiO*x* to SiN*y* were deposited by RF magnetron sputtering. FT-IR analysis revealed that the SiO*x*N*y* films deposited by co-sputtering silicon oxide and silicon nitride were composed of one homogeneous phase of random bonding O Si N network, *i.e.*, a structure interpreted by the RBM. Nanoindentation creep experiments on sputtered SiON films were conducted to investigate the time-dependent plastic deformation in the films at room temperature. The measured Young's modulus and indentation-hardness of SiON films were increased as the nitrogen content [N/(O + N)] increased in film composition. The creep behaviors of SiON films also illustrated a strong correlation with content of oxygen and nitrogen in composition. Upon nanoindentation creep, the plastic flow in high oxygen-containing SiON films (with a smaller value stress exponent) was more homogeneous than that of high nitrogen-containing SiON films (with a larger value stress exponent). A deformation mechanism established on the chemical bonding structure and STZ amorphous plasticity theory was proposed to explain the observed variations in creep response of SiON films.

Accomplishment/New Findings VII:
The Deformation of Microcantilever-Based Infrared Detectors during Thermal Cycling

Major Publication:
I-K Lin, Y. Zhang, and **X. Zhang**, "The Deformationof Microcantilever-Based Infrared Detectors during Thermal Cycling," *Journal of Micromechanics and Microengineering*, 18 (7) (2008) 075012.

Abstract:
Uncooled microcantilever-based infrared (IR) detectors have recently gained interest due to their low noise equivalent temperature difference (NETD), while concurrently maintaining low costs. These properties have made them available for a wider range of applications. However, the curvature induced by residual strain mismatch severely compromises the device's performance. Therefore, to meet performance and reliability requirements, it is important to fully understand the deformation of IR detectors. In this study, bimaterial (SiN*x*/Al) microcantilever-based IR detectors were fabricated using surface micromachining with polyimide as a sacrificial layer. Thermo-mechanical deformation mechanisms were studied through the use of thermal cycling. A temperature chamber with accurate temperature control and an interferometer microscope were adopted in this study for thermal cycling and full-field curvature measurements. It was found that thermal cycling reduced the residual strain mismatch within the bimaterial structure and thus flattened the microcantilever-based IR detectors. Specifically, thermal cycling with a maximum temperature of 295 °C resulted in a 97% decrease in curvature of the microcantilever-based IR detectors upon return to room temperature. The thermoelastic deformation of the IR detectors was modeled using both finite element method (FEM) and analytical methods. A modified analytical solution based on plate theory was established to describe the thermoelastic mechanical responses by using a correction factor derived from FEM. Although in the current study Al and SiN*x* were chosen for the application of microcantilever-based IR detectors, the general experimental protocol and modeling approach can be applied to describe thermoelastic mechanical responses of bimaterial devices with different materials. Toward the end of this paper, we studied the correction factors in the modified analytical solution while varying parameters such as Young's modulus ratio, thickness ratio and coefficient of thermal expansion (CTE) mismatch to investigate the influences of these parameters.

Selected Figures/Results:

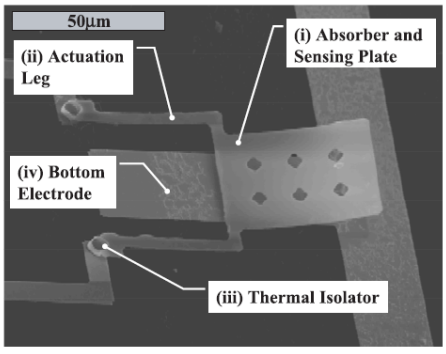

Fig. VII-1: SEM picture of the microcantilever-based IR detector consisting of four primary components: (i) IR radiation absorber, (ii) actuation legs, (iii) thermal isolator and (iv) bottom electrode.

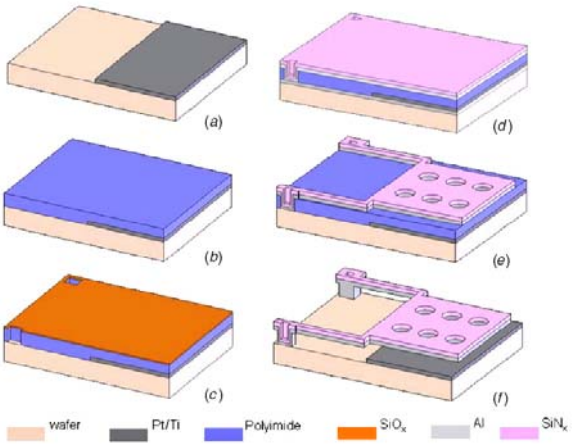

Fig. VII-2: Fabrication process flow of the microcantilever-based IR detector: (*a*) deposition of 150 nm thick Pt/Ti wires and pads by the standard lift-off process on silicon wafers, (*b*) spin-on coating and curing of 2.5 μm thick polyimide, (*c*) deposition of a 500 nm thick etching mask layer of PECVD SiO*x* and etching of SiO*x* and polyimide by RIE with SF6 and O2, respectively, (*d*) deposition of a 200 nm thick PECVD SiN*x* layer and a 200 nm thick e-beam evaporated Al layer, (*e*) patterning of SiN*x* and Al layers patterned using phosphoric acid and RIE with SF6 and He, respectively and (*f*) release of the cantilever by isotropic etching of polyimide layers with O2 plasma.

Deposition parameters of PECVD SiN_x film.

RF power	60 W
RF frequency	380 kHz
Pressure	550 mTorr
N_2 flow rate	1960 sccm
NH_3 flow rate	20 sccm
SiH_4 flow rate	40 sccm
Substrate temperature	300 °C
Deposition rate	7.87 Å s^{-1}

RIE etching parameters for PECVD SiO_x, PECVD SiN_x and polyimide film.

	SiF_6 (sccm)	He (sccm)	O_2 (sccm)	Pressure (mTorr)	Power (W)	Etching rate (nm min^{-1})
SiO_2	20	30	–	75	110	60.4
SiN_x	20	30	–	75	110	109
polyimide	–	–	40	100	300	870

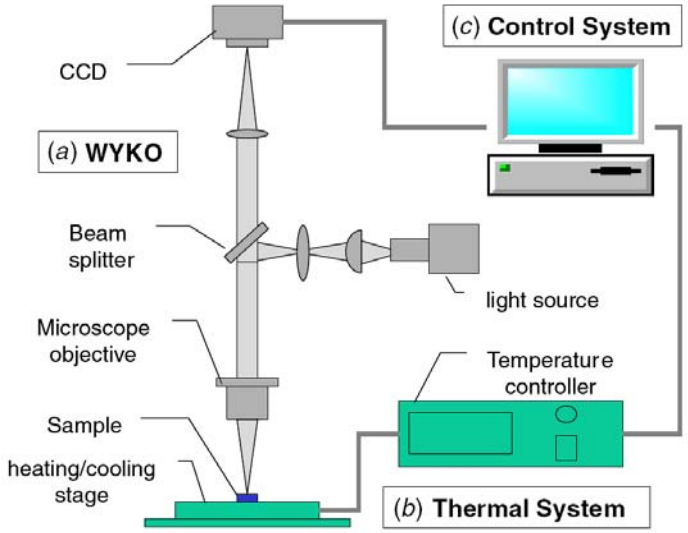

Fig. VII-3: Setup for *in situ* deformation measurement of the IR detector during thermal cycling: (*a*) WYKO interferometric microscope, (*b*) thermal system and (*c*) control system.

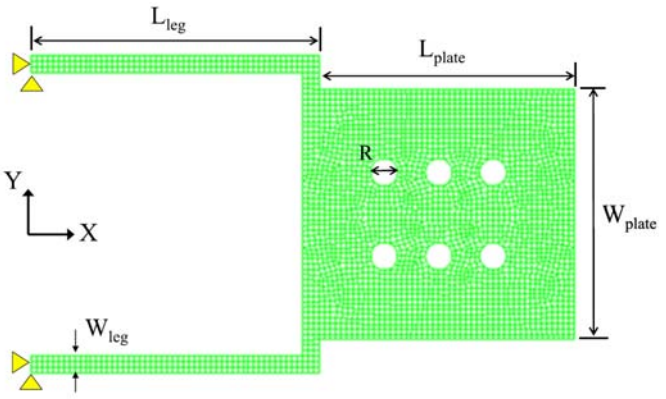

Fig. VII-4: Finite element mesh of the IR detector which was formed with two actuation legs and a sensing plate. The finite element model was constituted 2784 elements and 8859 nodes.

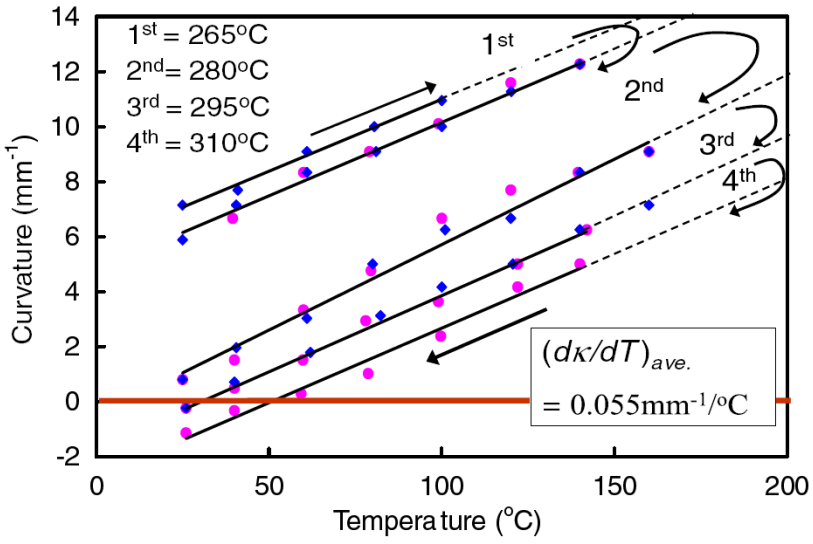

Fig. VII-5: Curvature versus temperature during the four thermal cycles with different peak temperatures (temperature increase, blue symbols; temperature decrease, pink symbols).

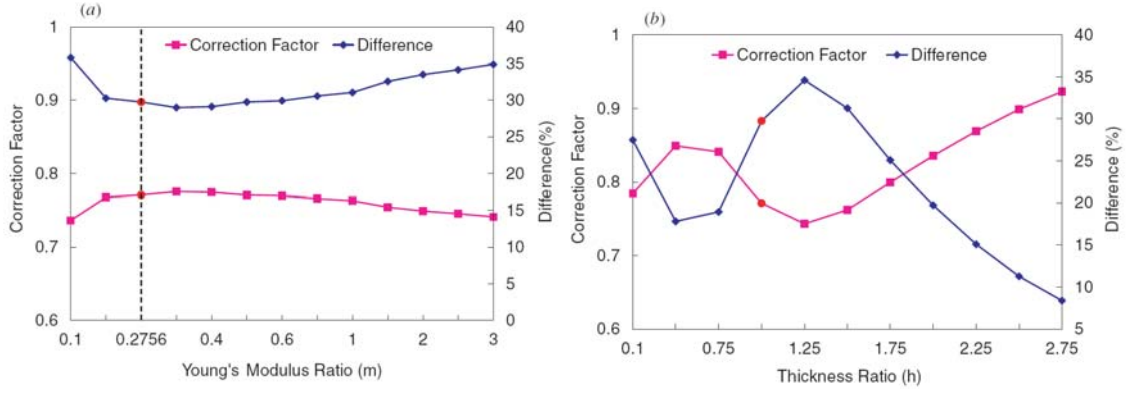

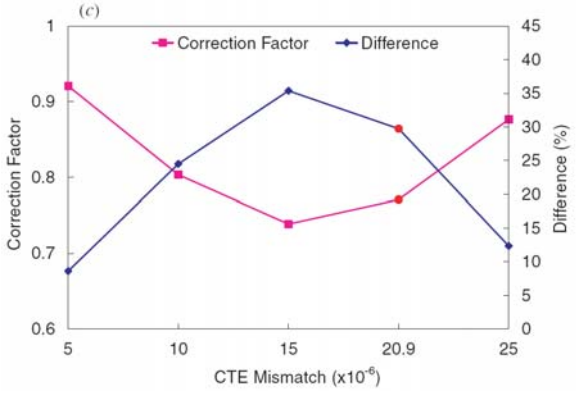

Fig VII-6: Correction factor and the percentage curvature difference varies as the parameters such as (*a*) Young's modulus ratio (*m*), (*b*) thickness ratio (*h*) and (*c*) mismatch of CTE ($\Delta\alpha$) change.

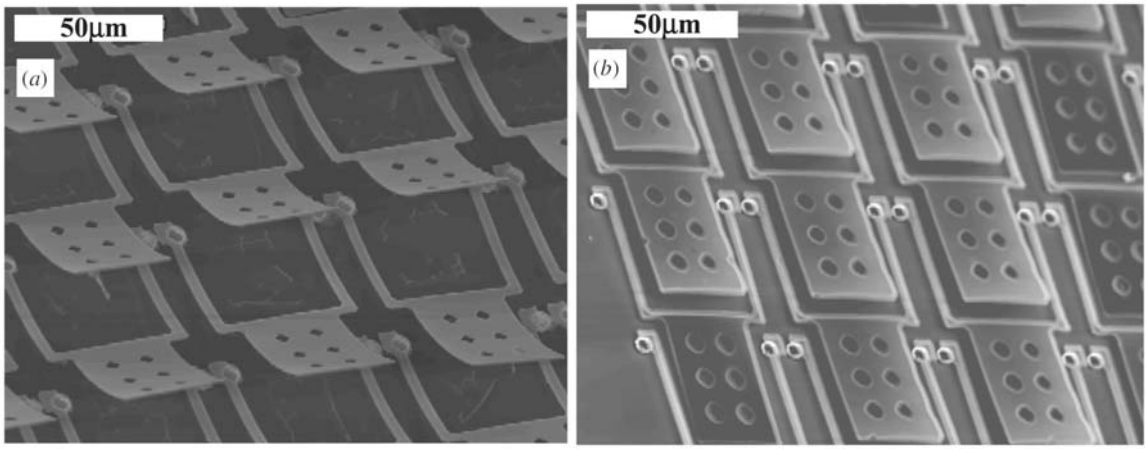

Fig. VII-7: SEM image of (*a*) as-released bimaterial SiN*x*/Al cantilever IR detectors which have residual strain mismatch induced curvature, (*b*) flattened IR detectors after thermal cycling with a peak temperature of 295 °C.

Concluding Remarks:

In this paper, a bimaterial microcantilever-based IR detector was fabricated using surface micromachining with a sacrificial polyimide layer. Thermal mechanisms were studied via thermal cycling to reduce the residual strain mismatch induced curvature of the microcantilever-based IR detectors. A thermal system and an interferometer were adopted to monitor the full-field curvature change *in situ*. Thermal cycling reduced the residual strain mismatch within the bimaterial device and thus flattened the microcantilever-based IR detectors. The linear thermoelastic mechanical response of the microcantilever-based IR detector was well described by using a modified analytical solution that employed a correction factor to modify present plate theory. The three critical parameters including Young's modulus ratio, thickness ratio and CTE mismatch were studied. Although bimaterial (SiN*x*/Al) microcantilever-based IR detectors are used in our design, this study can be generalized to other microcantilever-based IR detectors with different geometries and materials.

Accomplishment/New Findings VIII:
Thermomechanical Behavior and Microstructural Evolution of SiN*x*/***Al Bimaterial Microcantilevers***

Major Publication:
I-K Lin, Y. Zhang, and **X. Zhang**, "Thermomechanical Behavior and Microstructural Evolution of SiN*x*/Al Bimaterial Microcantilevers," *Journal of Micromechanics and Microengineering*, 19 (8) (2009) 085010.

Abstract:
Bimaterial microcantilevers are used in numerous applications in microelectromechanical systems (MEMS) for thermal, mechanical, optical, tribological and biological functionalities. Unfortunately, the residual stress-induced curvature and combined effects of creep and stress relaxation in the thin film significantly compromises the performance of these structures. To fully understand the themomechanical deformation and microstructural evolution of such microcantilevers, SiN*x*/Al bilayer cantilever beams were studied in this work. These microcantilevers were heated and subsequently cooled for five cycles between room temperature and 250 °C, with the peak temperature in each successive cycle increased in increments of 25 °C using a custom-built micro-heating stage. The *in situ* curvature change was monitored using an interferometric microscope. The general behavior of the biomaterial microcantilever beams can be characterized by linear thermoelastic regimes with $(d\kappa/dT)_{ave} = 0.079\ mm^{-1}\ {}^{\circ}C^{-1}$ and inelastic regimes. After thermal cycling with a maximum temperature of 225 °C, upon returning to room temperature, the bimaterial microcantilever beams were flattened and the curvature decreased by 99%. The thermoelastic deformation during thermal cycling was well described by the Kirchhoff plate theory. Deformation of biomaterial microcantilevers during long-term isothermal holding was studied at temperatures of 100 °C, 125 °C and 150 °C with a holding period of 70 h. The curvature of bimaterial microcantilever beams decreased more for higher holding temperatures. Finite element analysis (FEA) with power-law creep in Al was used to simulate the creep and stress relaxation and thus the curvature change of the bimaterial microcantilever beams. The microstructure evolutions due to isothermal holding in SiN*x*/Al microcantilevers were studied using an atomic force microscope (AFM). The grain growth in both the vertical and lateral directions was present due to isothermal holding. As the isothermal holding temperature increased, the surface roughness of the film increased with more prominent grain structures.

Selected Figures/Results:

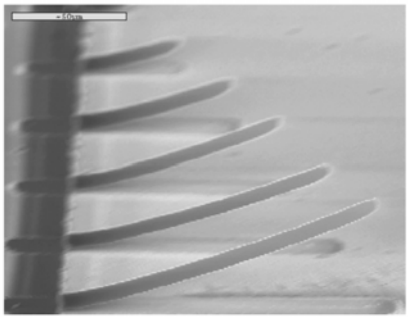

Fig. VIII-1: SEM image of an array of bimaterial SiN*x* (200 nm)/Al (200 nm) microcantilevers.

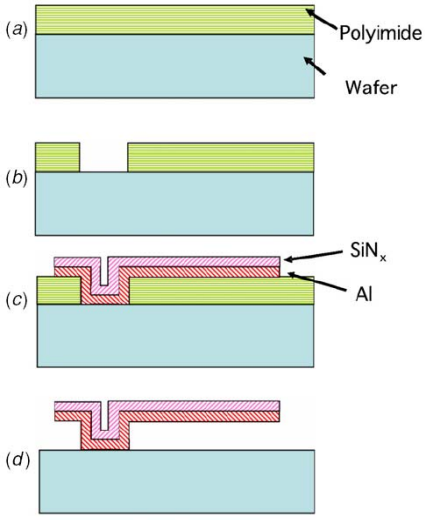

Fig. VIII-2: Fabrication process flow of SiN*x*/Al bimaterial microcantilevers.

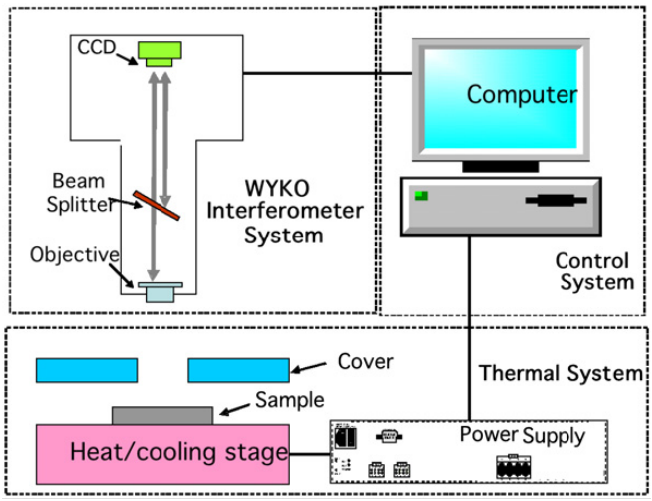

Fig. VIII-3: *In situ* deformation measurement setup consists of (*a*) WYKO interferometric microscope, (*b*) thermal system and (*c*) control system.

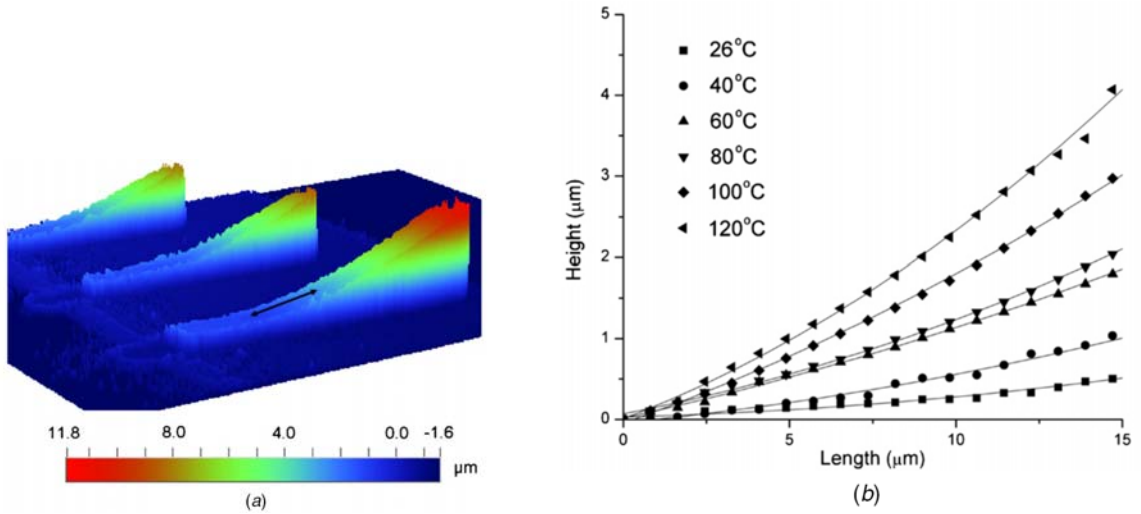

Fig. VIII-4: (*a*) Three-dimensional image of the as-fabricated microcantilever beams measured using the interferometer and (*b*) surface profiles of beam at different temperatures along the arrow line in (*a*).

Material parameters used in the finite element model.

	Young's modulus	Poisson's ratio	CTE	Thickness
SiN_x	254 Gpa	0.2	$2.1 \times 10^{-6}\ K^{-1}$	200 nm
Al	70 Gpa	0.3	$23 \times 10^{-6}\ K^{-1}$	200 nm

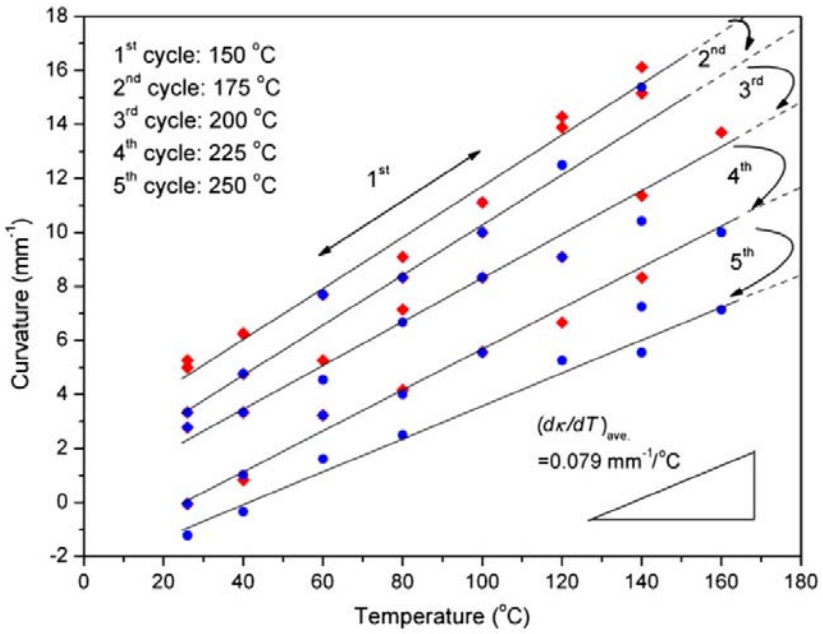

Fig. VIII-5: Curvature versus temperature for bimaterial SiN*x* (200 nm)/Al (200 nm) microcantilever beams during the five thermal cycles with different peak temperatures. The diamond and circle symbols are measured curvature during heating and cooling processes in each cycle, respectively.

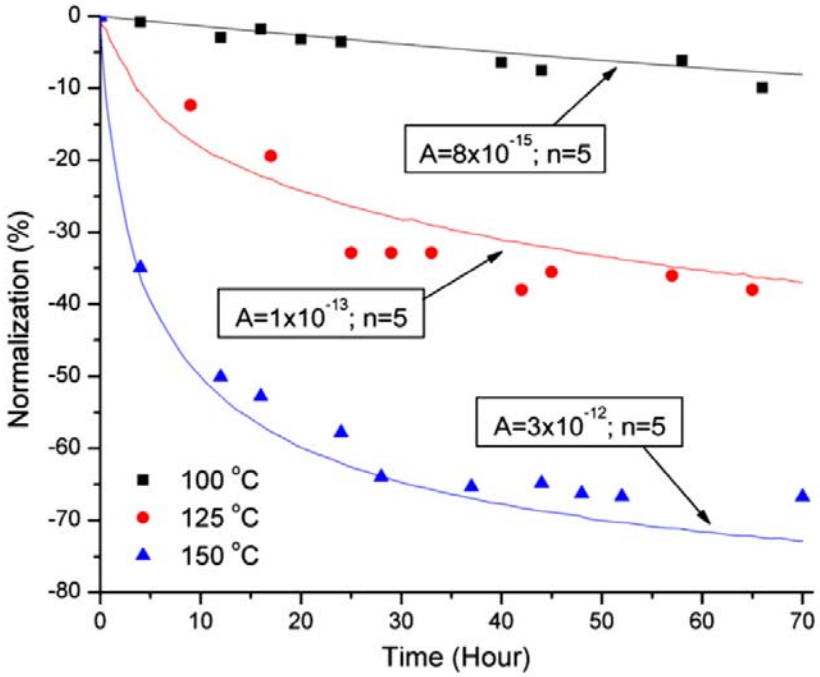

Fig. VIII-6: Measured and predicted curvature development during the 70 h of isothermal holding at 100, 120 and 150 °C for bilayer SiN*x*/Al microcantilever beams. The symbols represent experimental data while the solid lines represent predictions.

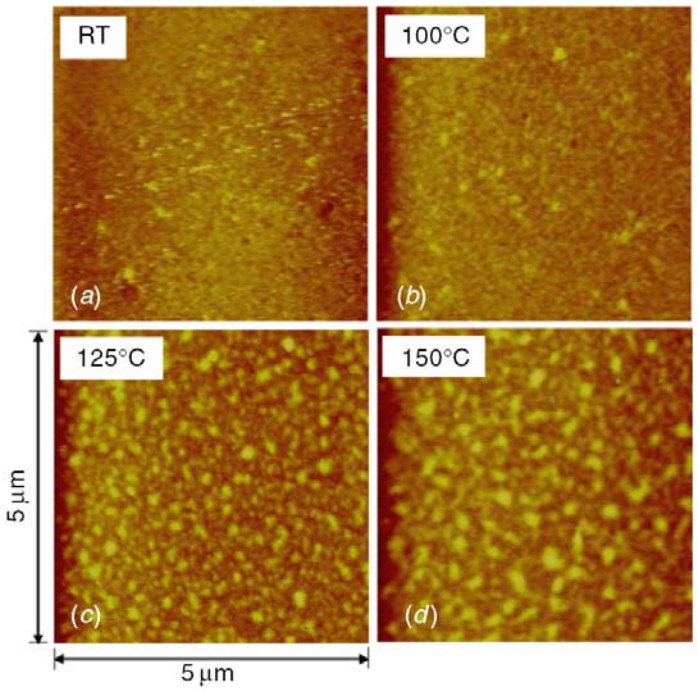

Fig. VIII-7: A series of AFM top-view images showing the grain growth on Al surface (*a*) before, and after 70 h isothermal holding at (*b*) 100 °C, (*c*) 125 °C and (*d*) 150 °C.

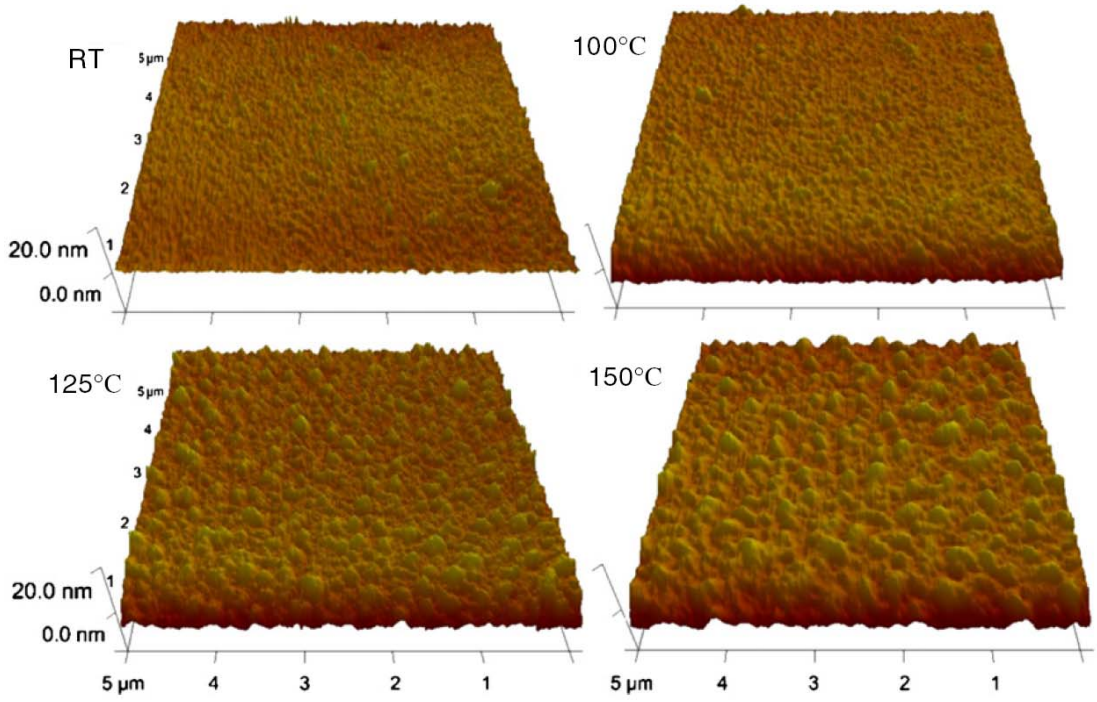

Fig. VIII-8: A series of AFM 3D images showing the grain growth on Al surface (*a*) before, and after 70 h isothermal holding at (*b*) 100 °C, (*c*) 125 °C and (*d*) 150 °C.

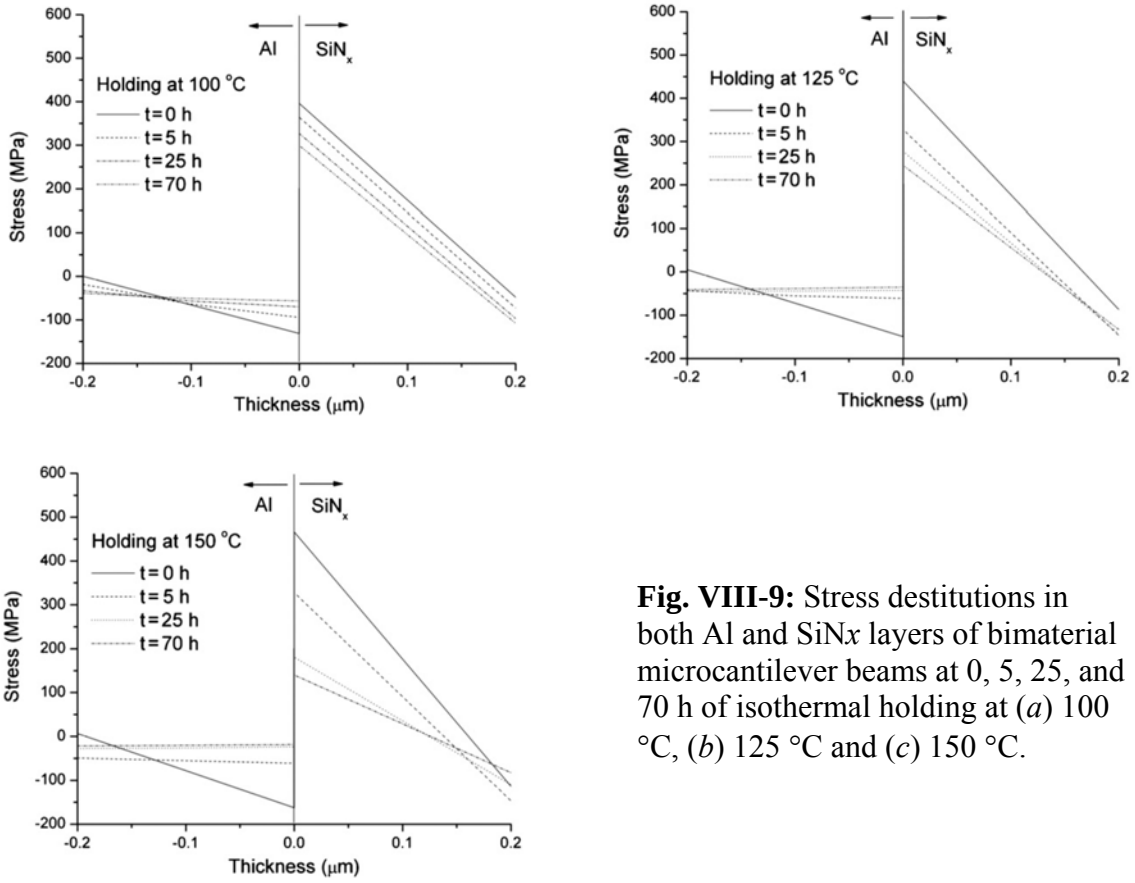

Fig. VIII-9: Stress destitutions in both Al and SiN*x* layers of bimaterial microcantilever beams at 0, 5, 25, and 70 h of isothermal holding at (*a*) 100 °C, (*b*) 125 °C and (*c*) 150 °C.

Concluding Remarks:

In this paper, SiN*x*/Al bimaterial microcantilevers were fabricated using surface micromachining with a sacrificial polyimide layer. A thermal system and an interferometric microscope were used to *in situ* measure the full-field out-of plane deformation of microcantilever beams. The deformation mechanisms with different thermal loading, including thermal cycling and isothermal holding were studied. Thermal cycling appears to be an effective method to modify the residual stress-induced curvature. Combined effects of creep and stress relaxation can greatly compromise the device performance, and can be simulated with power-law creep in Al to predict the curvature changes of the bimaterial microcantilevers. Moreover, morphology changes and grain growth of the Al surface were well captured using AFM, and was associated with the thermomechanical behavior and stress development of bimaterial microcantilevers. We would like to emphasize that the scope of this paper is not at all limited by IR detectors, which is only a specific application that could potentially benefit from this research. The scientific insights from this study contribute to the fundamental understanding of many other similar bilayer thin film material systems commonly used in MEMS. Broadly speaking, this paper would also help to identify more effective means for engaging the materials science and engineering mechanics community in work important to continuing advances in MEMS technology.

Supplement to VII and VIII:

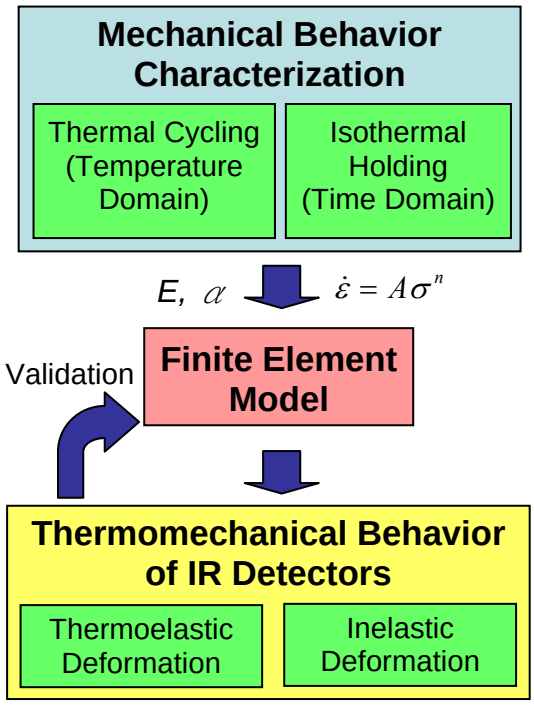

- Upon the thermomechanical response characterization on simple cantilever beams, the FEA model with characterized material parameter can be establish

- Thermal cycling on IR detectors
  - Thermal mechanical response (dk/dT)
  - Flatten IR detectors
  - Validate with the FEA model (elastic deformation)

- Isothermal holding on IR detectors
  - Validate with the FEA model
  - Predict the inelastic deformation

Summary:

- SiN*x*/Al bilayer microcantilevers were fabricated using surface micromachining with a sacrificial polyimide layer.
- The full-field thermal deformation of microcantilevers was *in-situ* measured by interferometer with micro-heating stage.
- Thermal cycling appears to be an effective method to modify the residual stress-induced curvature.
- Inelastic deformation during isothermal holding at various temperatures was fully characterized.
- Microstructural evolution in metal layer was observed.
- The FEM with characterized material properties was developed to predict thermal deformation of bilayer thin film cantilevers.

Accomplishment/New Findings IX:
The Tunability in Mechanical Properties and Fracture Toughness of Sputtered Silicon Oxynitride Thin Films for MEMS-based Infrared Detectors

Major Publication:
I-K Lin, P-H Wu, K-S Ou, K-S Chen, and **X. Zhang**, "The Tunability in Mechanical Properties and Fracture Toughness of Sputtered Silicon Oxynitride Thin Films for MEMS-based Infrared Detectors," *Thin Solid Films*, submitted/under review.

Abstract:
This paper presents the mechanical characterization of the elastic modulus, hardness and fracture toughness of silicon oxynitride films (SiON) with different oxygen and nitrogen content, subjected to thermal annealing processed at 400 °C and 800 °C. The Fourier-transform infrared (FT-IR) spectroscopy was employed to characterize the SiON films with respect to the absorbance peak in the infrared spectrum. The nanoindentation testing showed that both the elastic modulus and hardness slightly increased after thermal annealing. Finally, the fracture toughness of the SiON films were estimated using Vickers micro-indentation tests and the result revealed that the fracture toughness decreased with increasing rapid thermal annealing (RTA) temperature and nitrogen content. We believe these results benefit microelectromechanical systems (MEMS) in regards to maintaining the structural integrity and improving reliability performance.

Selected Figures/Results:

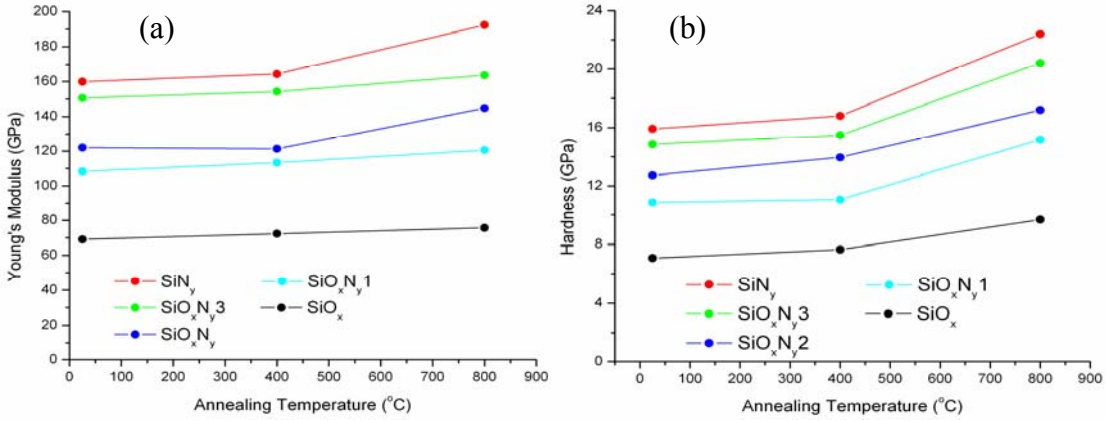

Fig. IX-1: The relationship between (a) elastic modulus and (b) hardness with respect to thermal annealing temperature.

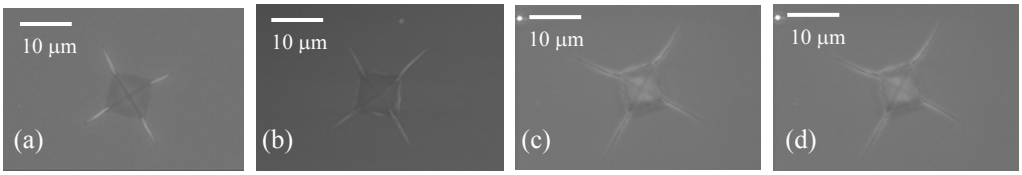

SiO_xN_y1 SiO_xN_y2 SiO_xN_y3 SiN_y

Fig. IX-2: The SEM image series of crack propagation for SiON films after 800 °C RTA.

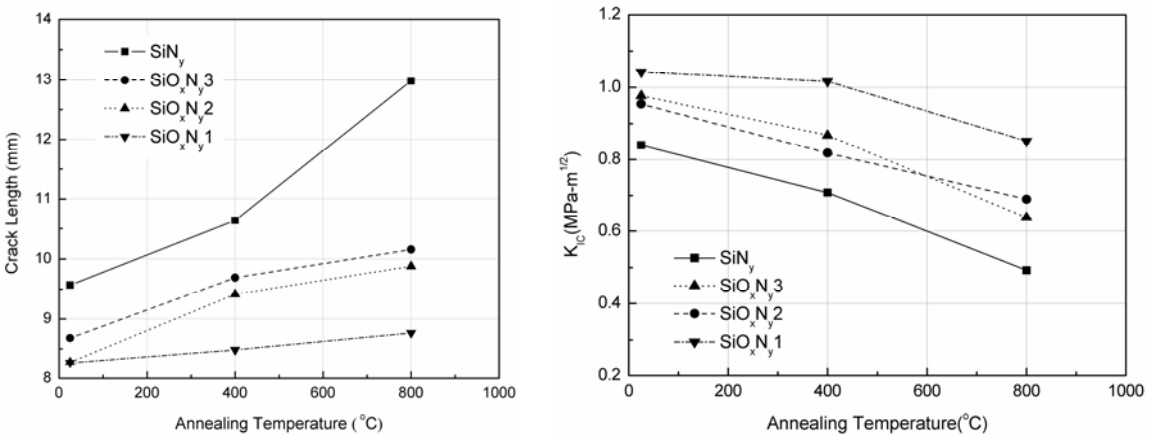

(a) (b)

Fig. IX-3: (a) The crack length and (b) fracture toughness of SiON films as a function of temperature.

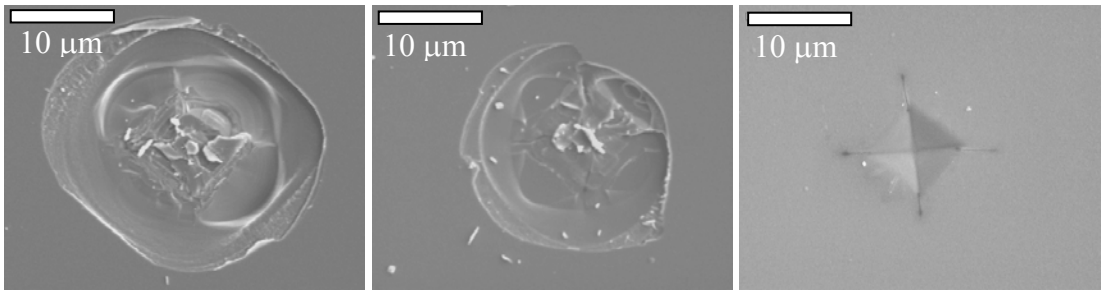

as-deposited after 400 °C annealing after 800 °C annealing

Fig. IX-4: SEM images of delamination on the SiO_x films after indentation.

Concluding Remarks:

Amorphous SiON films with varied composition of oxygen and nitrogen content ranging from SiO_x to SiN_y were deposited by RF magnetron sputtering. FT-IR analysis revealed that the absorbance peak of SiO_xN_y films is tunable by oxygen and nitrogen content ratio in films. Nanoindentation on sputtered SiON films was conducted to investigate the Young's modulus and hardness. The result shows that both Young's modulus and hardness of SiON films increases with increasing nitrogen content in films and thermal annealing temperature. On the other hand, the fracture toughness of SiON films decrease with increasing nitrogen content in films and thermal annealing temperature. The result provides useful information and reliability assessment for related MEMS and IC structure integrity design applications.

Accomplishment/New Findings X:
Thermomechanical Characterization and Modeling of Inelastic Deformation on Microcantilevers with Nanoscale Coating

Major Publication:
I-K Lin, Y. Zhang, and **X. Zhang**, "Thermomechanical Characterization and Modeling of Inelastic Deformation on Microcantilevers with Nanoscale Coating," *Journal of Micromechanics and Microengineering*, submitted/under review.

Abstract:
The application and commercialization of microelectromechanical system (MEMS) devices suffer from reliability problems due to the structural inelastic deformation during device operation. Nanocoating techniques, namely atomic layer deposition (ALD), have been demonstrated to be promising solutions for reliability problems in MEMS devices. However, the micro/nano- mechanics within and/or between microcantilevers and coatings are not fully understood, especially when temperature, time, microstructural evolution and material nonlinearities play significant roles in thermomechanical response. In this paper, the thermomechanical behavior of Au/SiN*x* bilayer microcantilevers are characterized by using thermal cycling and isothermal holding tests, as well as finite element analysis (FEA). A power law was used to emulate the mechanical behavior of microcantilevers during isothermal holding. After we found the constitutive law of Au, we developed a FEA model for inelastic deformation prediction on ALD alumina-coated microcantilever beams. The simulation results, however, do not agree with experimental results. This is because the ALD alumina alters the material parameters of constitutive law. After we modified the material constitutive law, the inelastic deformation of ALD alumina coated-microcantilevers became predictable again. Moreover, to better understand the stress relief and ALD alumina suppression mechanism, a scanning electron microscope (SEM) and atomic force microscope (AFM) were employed to explore the microstructural evolution. The method and results presented in this paper are believed to be useful for the fundamental understanding of many similar bilayer microcantilever-based MEMS devices.

Selected Figures/Results:

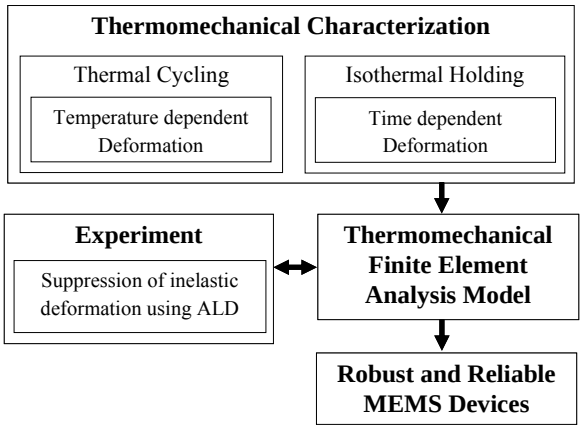

Fig. X-1: Overall research structure and process.

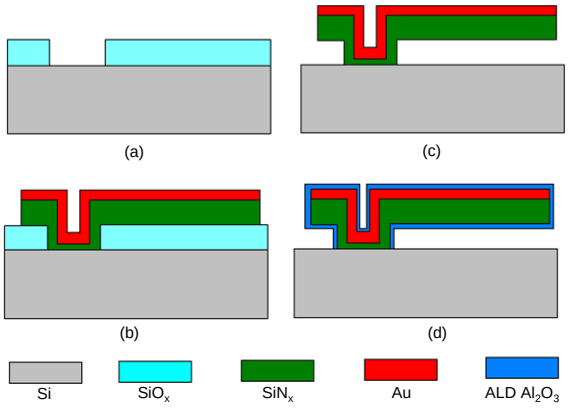

Fig. X-2: The schematic fabrication process flow of the Au/SiN*x* bilayer microcantilever beams with nanocoating: (a) deposition of 1.5 μm thick SiO_x and etching of SiO_x by RIE with SF6, (b) deposition of a 1.15 μm thick PECVD SiN*x* layer and a 0.5 μm thick e-beam evaporated Au layer, and patterning of Au and SiN*x* layers using KI and RIE with SF6 and He, respectively, (c) releasing of the microcantilever beams by isotropic etching of SiO_x with BOE and then drying by supercritical CO_2 release system, (d) nanocoating of 10 nm alumina by ALD.

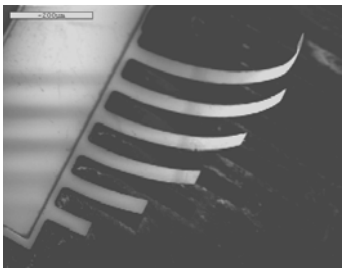

Fig. X-3: SEM image of an array of Au (0.5 μm thick)/SiN*x* (1.15 μm thick) microcantilever beams suspended over a silicon substrate.

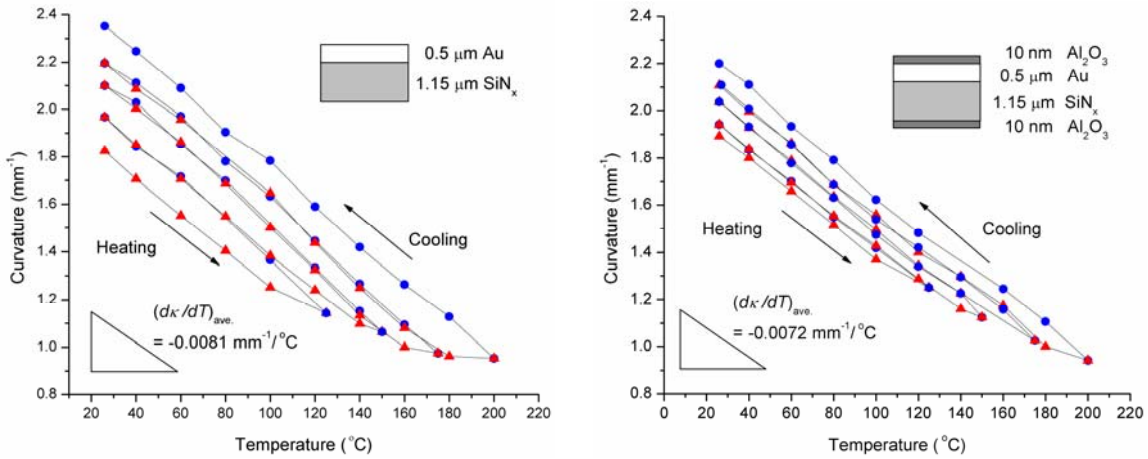

Fig. X-4: Curvature of (a) Au/SiN*x* microcantilever beams and (b) ALD alumina coated microcantilever beams as a function of temperature during 4 thermal cycles with different peak temperatures. The triangle and circle symbols are measured curvatures during the heating and cooling process in each cycle, respectively.

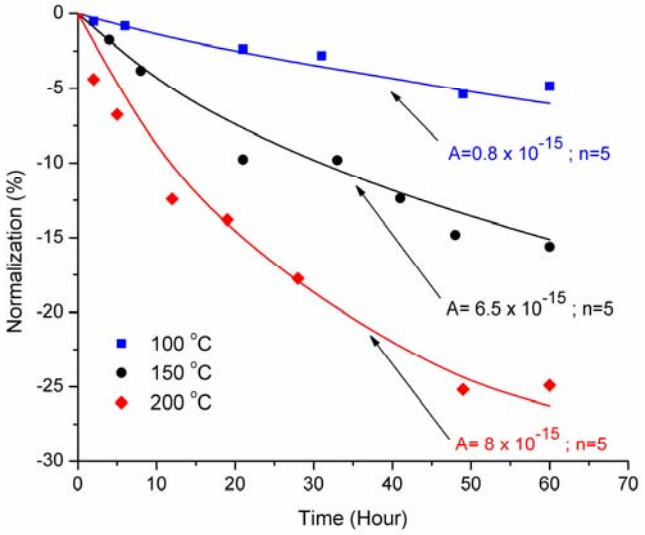

Fig. X-5: Curvature evolution during the 60 hours isothermal holding at 100 °C, 150 °C and 200 °C for Au/SiN*x* microcantilever beams. The symbols represent experimental data while the solid lines represent simulation results.

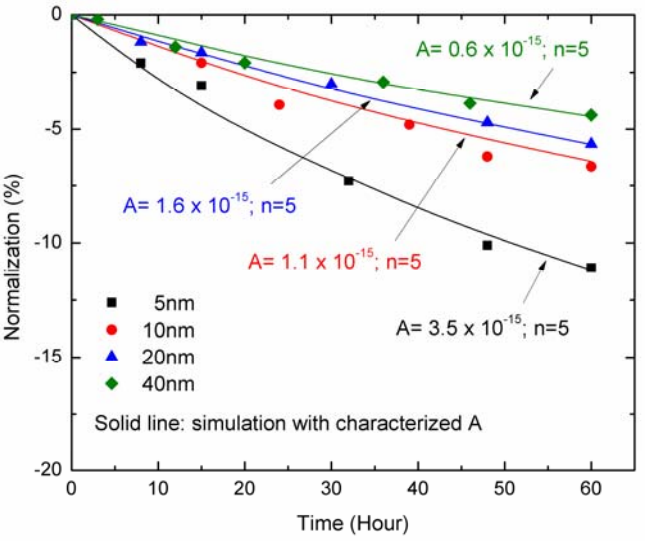

Fig. X-6: Curvature evolution during the 60 hours isothermal holding at 150 °C for 5 nm, 10 nm, 20 nm and 40 nm ALD alumina coated microcantilever beams. The symbols represent experimental data while the solid lines represent simulation results.

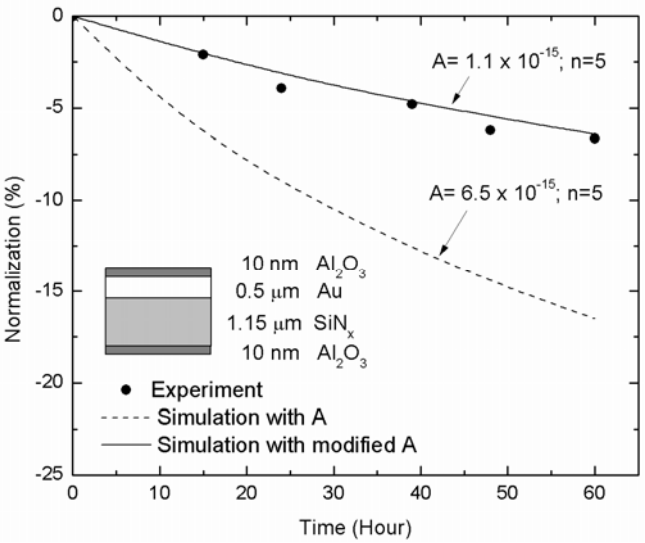

Fig. X-7: Experimental and simulation result of curvature evolution during the 60 hours isothermal holding at 150 °C for 10 nm ALD alumina coated Au/SiN*x* microcantilever beams. The symbols represent experimental data while the solid and dashed lines represent simulation results using different power laws.

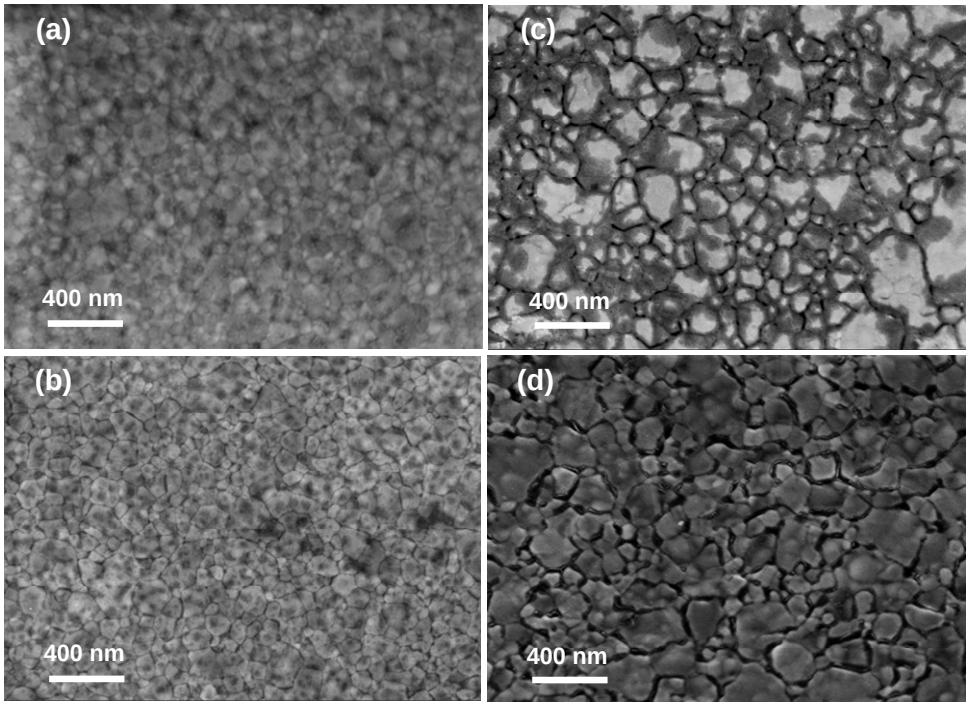

Fig. X-8: A series of SEM images of surface profiles on microcantilever beams (a) before and after 60 hours isothermal holding at (b) 100 °C, (c) 150 °C and (d) 200°C.

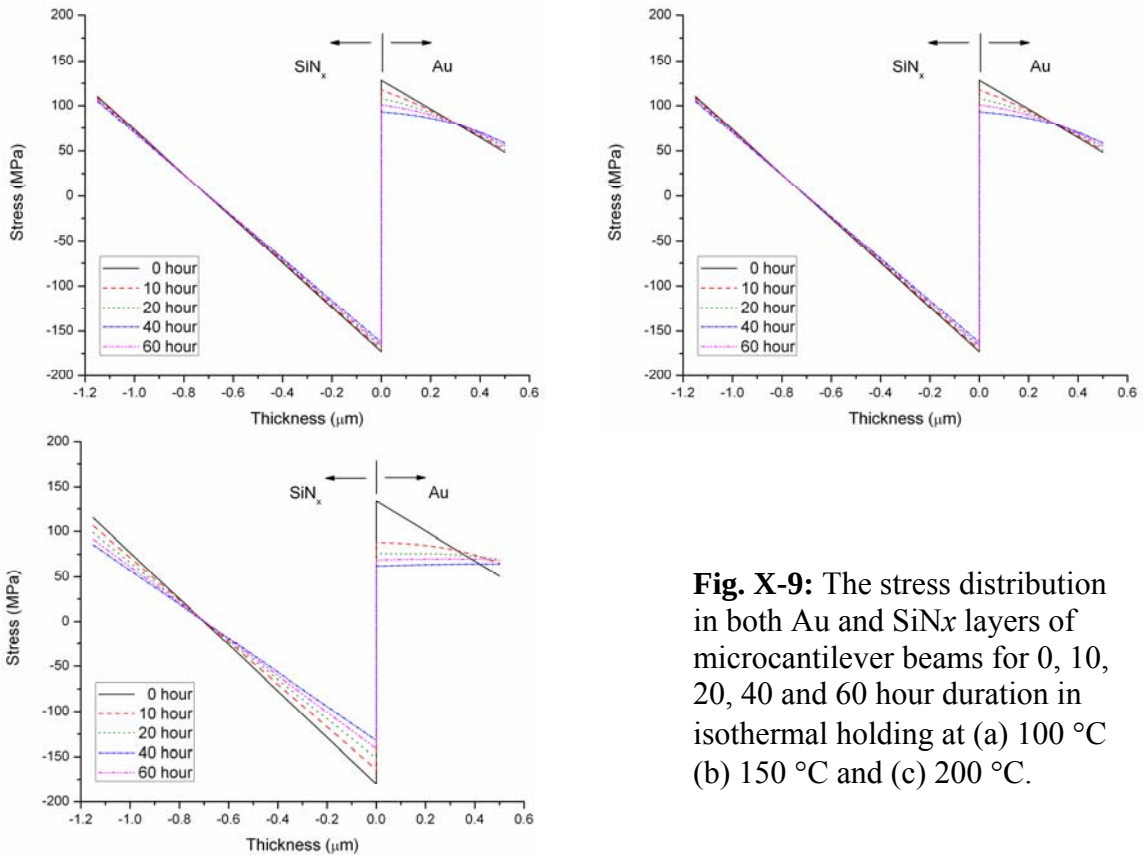

Fig. X-9: The stress distribution in both Au and SiN*x* layers of microcantilever beams for 0, 10, 20, 40 and 60 hour duration in isothermal holding at (a) 100 °C (b) 150 °C and (c) 200 °C.

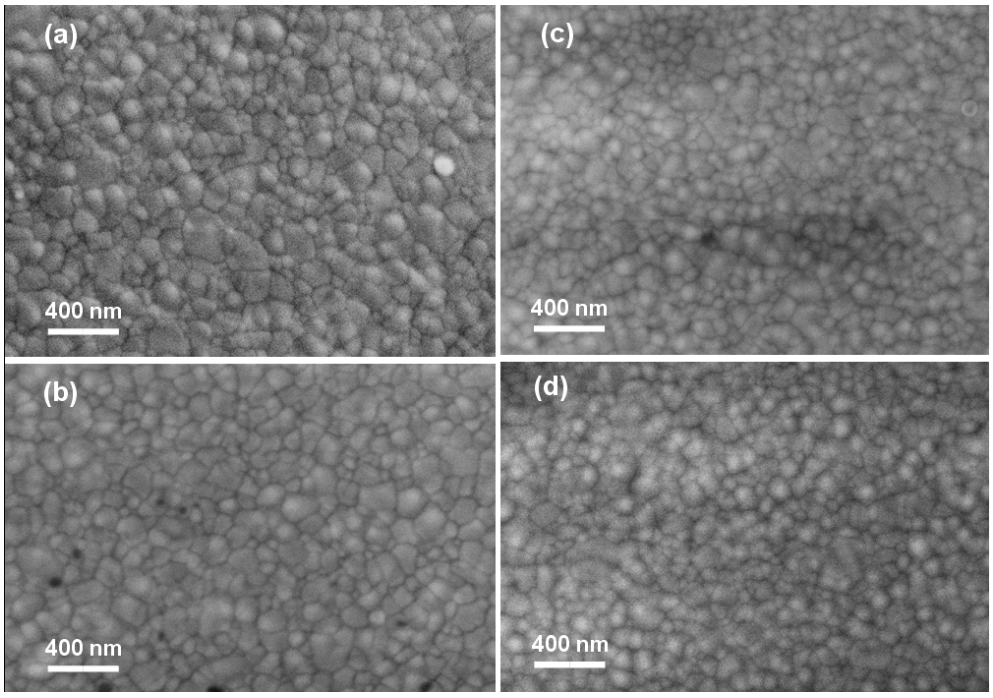

Fig. X-10: A series of SEM images of surface profile on (a) 5 nm, (b) 10 nm, (c) 20 nm and (d) 40 nm ALD alumina coated microcantilever beams after 60 hours of isothermal holding at 150 °C.

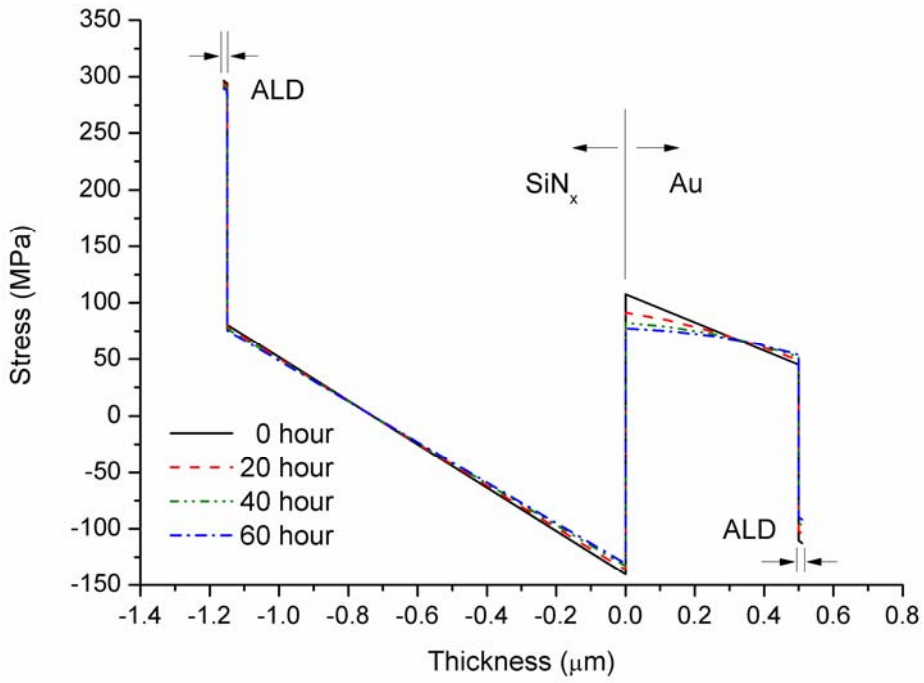

Fig. X-11: The stress distribution in 10 nm ALD alumina, Au and SiN*x* layers of ALD coated microcantilever beams for 0, 10, 20, 40 and 60 hour duration in isothermal holding at 150 °C.

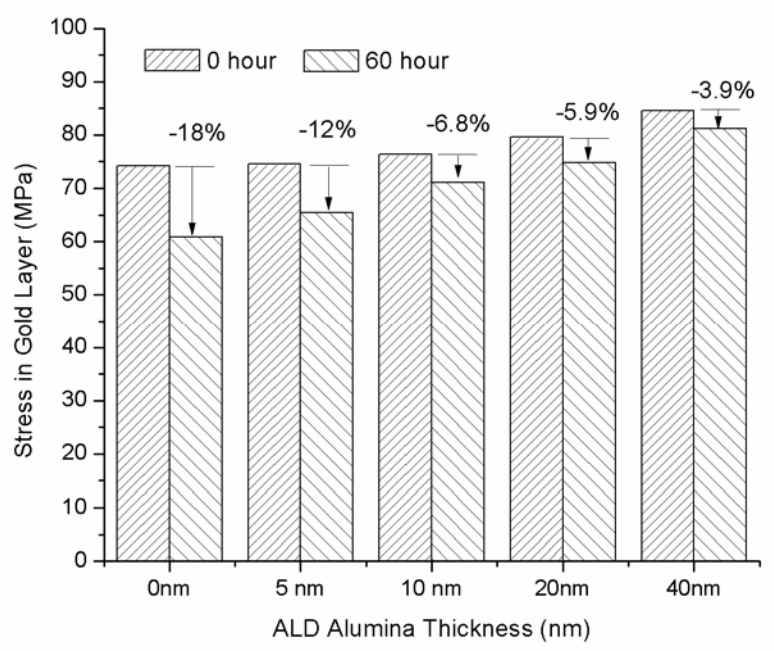

Fig. X-12: The relationship between ALD alumina thicknesses and tensile stress relief in Au layer after 150 °C isothermal holding.

Concluding Remarks:

The understanding and modeling of the thermomechanical behavior of coated and uncoated microcantilevers, including temperature and time- dependent deformation, is critical to the acquisition of the robust and reliable MEMS structures and devices for the next generation. In this paper, we demonstrated a comprehensive thermomechanical characterization using thermal cycling and isothermal holding, as well as developed a FEA model with an appropriate material constitutive law to predict the inelastic deformation on Au/SiN*x* bilayer microcantilever beams. The ALD alumina nanocoating successfully suppressed the inelastic deformation but the simulation results of inelastic deformation do not agree well with experimental results. This is because the ALD alumina alters the material parameters of the constitutive law. After modifying the material constitutive law, the inelastic deformation of ALD alumina-coated microcantilevers is predictable again. Moreover, to better understand the stress relief and ALD alumina suppression mechanism, a scanning electron microscope (SEM) and atomic force microscope (AFM) were employed to explore the microstructural evolution. The scientific insights from the in-depth study of thermomechanical behavior of ALD alumina-coated and uncoated Au/SiN*x* bilayer microcantilever beams also contributes to the fundamental understanding and analysis of similar thermomechanical responses of similar microcantilevers commonly used in MEMS.

Acknowledgement:

- Dr. Les Lee, AFOSR
- All of Members at Boston University Laboratory for Microsystems Technology (LMST)
- The Photonics Center at Boston University
- Fraunhofer Center for Manufacturing Innovation
- Boston University Division of Materials Science and Engineering
- Boston University Center of Nanoscience and Nanotechnology